JEM Journal of Experimental Medicine

ARTICLE

PMN-derived netrin-1 attenuates cardiac ischemia-reperfusion injury via myeloid ADORA2B signaling

Jiwen Li[1,2], Catharina Conrad[1,3], Tingting W. Mills[4], Nathaniel K. Berg[1], Boyun Kim[1], Wei Ruan[1,5], Jae W. Lee[6], Xu Zhang[7], Xiaoyi Yuan[1], and Holger K. Eltzschig[1]

Previous studies implicated the neuronal guidance molecule netrin-1 in attenuating myocardial ischemia-reperfusion injury. However, the tissue-specific sources and receptor signaling events remain elusive. Neutrophils are among the first cells responding to an ischemic insult and can be associated with tissue injury or rescue. We found netrin-1 levels were elevated in the blood of patients with myocardial infarction, as well as in mice exposed to myocardial ischemia-reperfusion. Selectively increased infarct sizes and troponin levels were found in *Ntn1*$^{loxP/loxP}$ Lyz2 Cre^{+} mice, but not in mice with conditional netrin-1 deletion in other tissue compartments. In vivo studies using neutrophil depletion identified neutrophils as the main source for elevated blood netrin-1 during myocardial injury. Finally, pharmacologic studies using treatment with recombinant netrin-1 revealed a functional role for purinergic signaling events through the myeloid adenosine A2b receptor in mediating netrin-1–elicited cardioprotection. These findings suggest an autocrine signaling loop with a functional role for neutrophil-derived netrin-1 in attenuating myocardial ischemia-reperfusion injury through myeloid adenosine A2b signaling.

Introduction

Myocardial infarction (MI) remains a leading health problem, causing millions of deaths each year worldwide (Heusch, 2020; Yellon and Hausenloy, 2007). Early revascularization to restore the blood supply of the infarcted myocardium is critical to limit tissue injury and subsequent dysfunction. However, the reperfusion process itself may induce further injury, which contributes up to 50% of the final infarct size (Hausenloy and Yellon, 2013). Different disease mechanisms contribute to reperfusion injury, including calcium overload, oxidative stress, mitochondrial dysfunction, and excessive immune cell infiltration. Particularly the infiltration of neutrophils has been implicated in exacerbating myocardial injury during reperfusion due to the release of cytotoxic mediators (Bonaventura et al., 2016; Hausenloy et al., 2017; Kalogeris et al., 2012). Effective approaches targeting the reduction of myocardial ischemia-reperfusion (IR) injury are lacking, and novel therapeutic options are urgently needed.

Neuronal guidance proteins (NGPs) are a family of proteins originally studied for nervous system development. By guiding through chemoattractive and chemorepulsive signals, NGPs drive the axon cone outgrowth to the proper destinations and form the intricate neural circuit (Guan and Rao, 2003; Van Battum et al., 2015). More recently, NGPs have also been implicated in guiding immunological responses (Mirakaj and Rosenberger, 2017). One of the most studied NGPs in the context of inflammation is netrin-1, which has been found to have important immunological functions by guiding inflammatory events, particularly during conditions of limited oxygen availability (hypoxia). For example, studies show that netrin-1 can function to dampen hypoxia-driven inflammation of different organs (Rosenberger et al., 2009) during intestinal inflammation (Aherne et al., 2012) or during IR injury (Grenz et al., 2011a). Netrin-1 signaling traditionally involves deleted in colorectal cancer receptor (DCC) or the uncoordinated-5 (UNC5) homologues UNC5A, B, C, and D receptors (Moore et al., 2007). However, recent studies have implicated the adenosine A2b receptor (ADORA2B) in mediating the anti-inflammatory roles

[1]Department of Anesthesiology, The University of Texas Health Science Center at Houston, McGovern Medical School, Houston, TX; [2]Department of Cardiac Surgery, Sir Run Run Shaw Hospital, School of Medicine, Zhejiang University, Hangzhou, China; [3]Department of Anesthesiology, Intensive Care and Pain Medicine, University Hospital Münster, Münster, Germany; [4]Department of Biochemistry and Molecular Biology, The University of Texas Health Science Center at Houston, Houston, TX; [5]Department of Anesthesiology, Second Xiangya Hospital, Central South University, Hunan, China; [6]Department of Anesthesiology, Yale University School of Medicine, New Haven, CT; [7]Center for Clinical and Translational Sciences, The University of Texas Health Science Center at Houston, Houston, TX.

Correspondence to Holger K. Eltzschig: holger.eltzschig@uth.tmc.edu.

of netrin-1. The first evidence that netrin-1 can interact with the ADORA2B comes from studies using a two-hybrid screen of a human brain cDNA library using the intracellular domain of DCC as bait (Corset et al., 2000). Additional work suggested that ADORA2B can function as a netrin-1 receptor, indicating that the growth-promoting function of netrin-1 requires a receptor complex containing DCC and ADORA2B (Corset et al., 2000). While there have been conflicting findings on the ADORA2B–netrin-1 interaction (Moore et al., 2007; Stein et al., 2001), several studies corroborate ADORA2B as the netrin receptor responsible for attenuating inflammation and neutrophil trafficking during hypoxia (Aherne et al., 2012; Feinstein and Ramkhelawon, 2017; Layne et al., 2015; Mirakaj et al., 2010; Rosenberger et al., 2009).

Previous studies provide evidence that netrin-1 can dampen myocardial IR injury (Mao et al., 2014; Zhang and Cai, 2010). However, the tissue-specific contributions for netrin-1 and the receptor signaling events remain unclear. Studying netrin-1 biology using genetic models has been complicated by the fact that mice with homozygous netrin-1 deletion die shortly after birth due to severe brain defects (Serafini et al., 1996). Thus, we generated a transgenic mouse with a "floxed" *netrin-1* gene (Brunet et al., 2014; Hadi et al., 2018; Zhu et al., 2019) that allowed us to achieve specific deletion of netrin-1 in different tissue compartments. Our studies indicate that myeloid-derived netrin-1 plays a central role in attenuating myocardial IR injury through interacting with the ADORA2B expressed on inflammatory cells.

Results

Blood netrin-1 is increased in patients with MI and in mice with myocardial IR injury

Previous reports implicated netrin-1 in hypoxia adaptation (Rosenberger et al., 2009) and protection during myocardial IR injury (Rosenberger et al., 2009; Zhang and Cai, 2010). However, studies in genetic models or studies addressing tissue-specific functions in netrin-elicited cardioprotection have yet to be reported. Here, we hypothesized that soluble netrin-1 could have a functional role in attenuating myocardial IR injury. As a first step to address this hypothesis, we measured the levels of circulating netrin-1 in the blood from patients who experienced MI compared with healthy control subjects using ELISA. Corresponding cardiac troponin I (cTnI) levels of patients with MI were documented in the patient sample data sheet (Table S1 and Table S2). Consistent with our hypothesis, we found elevated levels of blood netrin-1 in patients with MI compared with healthy control subjects (Fig. 1 A; $n = 10$ for healthy donor group; $n = 9$ for MI group). Due to our small patient cohort, the correlation between netrin-1 and troponin levels was not conclusive. To determine if the blood netrin-1 elevations were consistent with a murine myocardial IR model, we ligated the left coronary artery (LCA) of C57BL/6 mice (WT) to achieve 45 min of myocardial ischemia and 120 min of reperfusion. A sham group underwent a similar procedure without applying weights to ligate the coronary artery (Fig. 1 B). Mice exposed to myocardial IR demonstrated significant myocardial injury, measured by the gross presence of infarcted tissue staining and elevated blood troponin levels (Fig. 1, C–E). Consistent with the above studies in patients experiencing MI, mice exposed to myocardial IR showed significant elevations of blood netrin-1 levels. Compared with ischemia alone or with 4 h of reperfusion, blood netrin-1 levels significantly increased after 45 min of ischemia and 2 h of reperfusion (Fig. 1 F), but the netrin-1 protein levels of heart tissue did not change significantly (Fig. S1, A and B). Notably, there were no significant sex differences in murine blood netrin-1 levels (Fig. S1, C and D). Taken together, these studies demonstrate that levels of circulating netrin-1 are elevated in the blood following myocardial IR injury in both humans and mice.

Ntn1$^{loxP/loxP}$ Lyz2 Cre^{+} mice demonstrate worsened myocardial IR injury

After having shown that blood netrin-1 levels are elevated following myocardial injury, we next set out to determine the tissue-specific origins of circulating netrin-1 and the role of netrin-1 in cardioprotection. To gain insight into the tissue distribution of netrin-1, we performed netrin-1 immunohistochemistry in mouse hearts that were subjected to IR injury. Positive netrin-1 staining was observed predominantly within cardiomyocytes and in circulating white blood cells representing primarily neutrophils based on their histological appearance (Fig. S2 A). We performed netrin-1 immunofluorescence costaining with a cardiomyocyte marker (cTnT) and a neutrophil marker (Ly6G), which further confirmed the cellular netrin-1 sources (Fig. 1 G; negative controls, see Fig. S2 B). Therefore, we generated transgenic mice with tissue-specific deletion of netrin-1 using the Cre-lox system. We generated *Ntn1*$^{loxP/loxP}$ Myosin Cre^{+} and *Ntn1*$^{loxP/loxP}$ Lyz2 Cre^{+} mice to knock down netrin-1 in cardiomyocytes or within the myeloid compartment, respectively (Fig. S3, A and B). *Ntn1*$^{loxP/loxP}$ Myosin Cre^{+} mice failed to show significantly altered myocardial infarct sizes or troponin levels as compared with Myosin Cre^{+} control animals (Fig. 2, B–D). In contrast, *Ntn1*$^{loxP/loxP}$ Lyz2 Cre^{+} mice demonstrated significantly larger infarct sizes (Fig. 2, E and F) and elevated troponin levels ($P = 0.006$; Fig. 2 G) as compared with Lyz2 Cre^{+} control mice. In conclusion, these studies provide the first evidence for a functional role for myeloid-derived netrin-1 in providing cardioprotection from IR injury.

Neutrophils contribute to increased blood netrin-1 levels during myocardial IR

After observing the phenotype of mice with myeloid-specific deletion of netrin-1 (*Ntn1*$^{loxP/loxP}$ Lyz2 Cre^{+}), we subsequently measured blood netrin-1 levels in *Ntn1*$^{loxP/loxP}$ Lyz2 Cre^{+} or Lyz2 Cre^{+} controls following IR. Blood netrin-1 increased significantly after IR in Lyz2 Cre^{+} mice, but not in *Ntn1*$^{loxP/loxP}$ Lyz2 Cre^{+} mice (Fig. 3, A and B). Neutrophils are among the first cells responding to an ischemic insult and represent the predominant cell population in the murine peripheral blood (O'Connell et al., 2015). Therefore, we hypothesized that neutrophils could be an important source for elevated circulating netrin-1 levels during IR, although it has to be taken into account that Lyz2 Cre-mediated conditional gene deficiency also targets monocytes and macrophages (Clausen et al., 1999). To investigate this

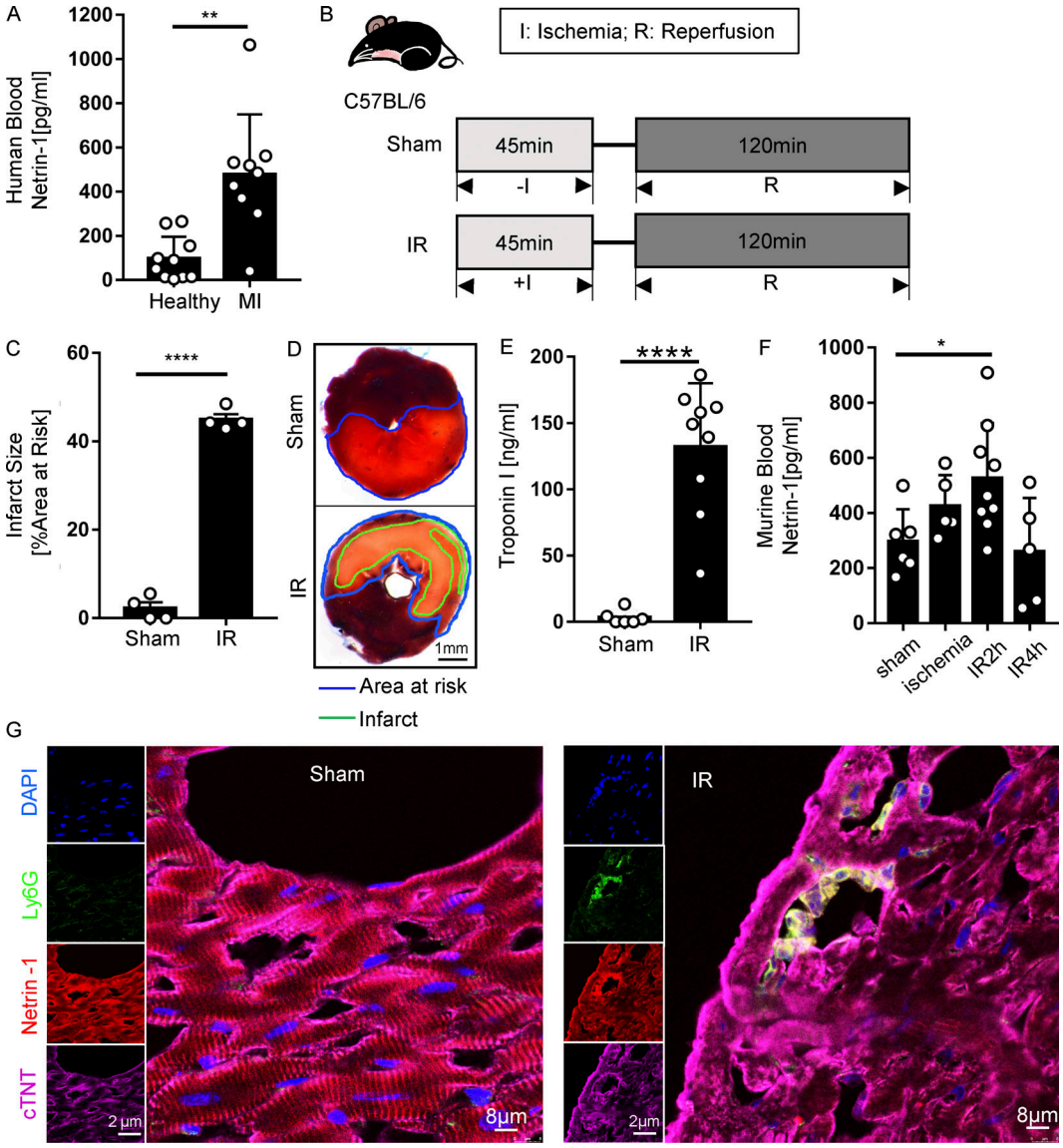

Figure 1. **Blood netrin-1 increases in MI patients and mice with myocardial IR surgery. (A)** Blood netrin-1 levels of healthy donors and MI patients (n = 10 for healthy control, n = 9 for MI; two-tailed Welch's t test). **(B)** Experimental strategy for the murine myocardial IR model. **(C)** Infarct sizes of IR group compared with the sham group (n = 4 per group; two-tailed unpaired t test). **(D)** Representative infarct staining results for the IR model. The infarct area is outlined by a green line; the blue line marks the AAR (scale bar = 1 mm). **(E)** cTnI levels after surgery (n = 6 for sham group, n = 9 for IR group; two-tailed Welch's t test). **(F)** Murine blood netrin-1 levels were measured in sham, ischemia (45 min), IR2h (45 min of ischemia + 2 h of reperfusion), and IR4h (45 min of ischemia + 4 h of reperfusion) groups (n = 6 for sham group, n = 5 for ischemia group, n = 9 for IR2h group, and n = 5 for IR4h group; one-way ANOVA with Bonferroni post hoc tests). **(G)** Immunofluorescence costaining of netrin-1 with cTnT and Ly6G in WT mice after sham or IR surgery shows netrin-1 in cardiomyocytes and neutrophils. (For single-channel pictures, scale bar = 2 μm; for merged channel pictures, scale bar = 8 μm.) *, P < 0.05; **, P < 0.01; ****, P < 0.0001. Data are presented as mean ± SD.

hypothesis, we performed antibody-based neutrophil depletion before sham or IR surgery and subsequently measured blood netrin-1 levels (Fig. 3, C and D). Consistent with our hypothesis, we found that neutrophil depletion was associated with diminished elevations of blood netrin-1 levels when compared with the isotype IgG controls (Fig. 3 E). In contrast, blood netrin-1 levels continued to be elevated after IR in mice that underwent clodronate-mediated monocyte/macrophage depletion (Fig. S2, D and E). In addition, we observed increased netrin-1 levels in the conditioned supernatant from human polymorphonuclear neutrophils (PMNs) activated with either TNFα or N-Formylmethionine-leucyl-phenylalanine (fMLP; PBS or DMSO as control, respectively) for 2 h. Consistent with the above in vivo studies, we found that human PMNs released high levels of netrin-1 into their supernatant following in vitro activation by TNFα or fMLP (Fig. 3, F and G). Previous studies described surface netrin-1 staining on myeloid cells, such as macrophages (Berg et al., 2021). To gain insight into the intracellular distribution of netrin-1, we costained netrin-1 and human PMN granular protein lysozyme, a protein that is widely stored in three types of neutrophil granules (Faurschou and Borregaard, 2003). These studies indicate that netrin-1 is

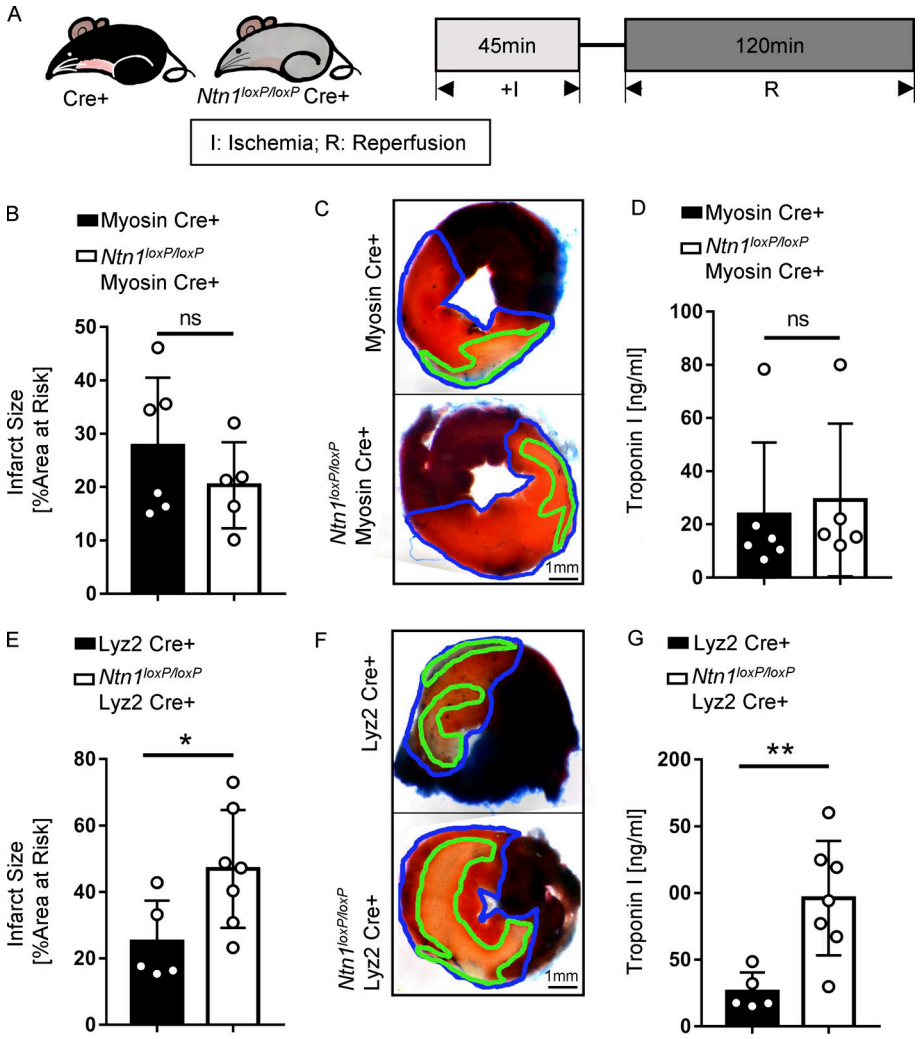

Figure 2. ***Ntn*$^{loxP/loxP}$ Lyz2 Cre^{+} mice have severe injury after myocardial IR surgery. (A)** Experimental strategy for myocardial IR model. **(B)** Infarct sizes of Myosin Cre^{+} mice compared with *Ntn1*$^{loxP/loxP}$ Myosin Cre^{+} mice after IR surgery (n = 6 for Myosin Cre^{+}, n = 5 for *Ntn1*$^{loxP/loxP}$ Myosin Cre^{+}; two-tailed unpaired t test). **(C)** Representative infarct staining results of Myosin Cre^{+} mice and *Ntn1*$^{loxP/loxP}$ Myosin Cre^{+} mice. The infarct area is outlined by a green line, and the blue line marks the AAR (scale bar = 1 mm). **(D)** cTnI levels of Myosin Cre^{+} mice compared with *Ntn1*$^{loxP/loxP}$ Myosin Cre^{+} mice after surgery (n = 6 for Myosin Cre^{+}, n = 5 for *Ntn1*$^{loxP/loxP}$ Myosin Cre^{+}; Mann-Whitney test). **(E)** Infarct sizes of Lyz2 Cre^{+} mice compared with *Ntn1*$^{loxP/loxP}$ Lyz2 Cre^{+} mice after IR surgery (n = 5 for Lyz2 Cre^{+}, n = 7 for *Ntn1*$^{loxP/loxP}$ Lyz2 Cre^{+}; two-tailed unpaired t test). **(F)** Representative infarct staining results of Lyz2 Cre^{+} mice and *Ntn1*$^{loxP/loxP}$ Lyz2 Cre^{+} mice as described in C (scale bar = 1 mm). **(G)** cTnI levels of Lyz2 Cre^{+} mice compared with *Ntn1*$^{loxP/loxP}$ Lyz2 Cre^{+} mice after surgery (n = 5 for Lyz2 Cre^{+}, n = 7 for *Ntn1*$^{loxP/loxP}$ Lyz2 Cre^{+}; two-tailed unpaired t test). *, P < 0.05; **, P < 0.01. Data are presented as mean ± SD.

predominantly contained within the cytosol but not in the lysozyme-containing granules (Fig. 3 H; negative controls, see Fig. S2 C). Taken together, these findings implicate neutrophils as a source for increased blood netrin-1 levels during cardiac IR injury and concomitant cardioprotection.

Cardioprotection of netrin-1 is ADORA2B dependent

After demonstrating that netrin-1 is released into the circulation by PMNs, resulting in cardioprotection from IR injury, we next pursued studies to address the involvement of netrin-1 signaling events. Previous studies had shown that netrin-1 can function to dampen hypoxia-driven inflammation by enhancing purinergic signaling events (Eckle et al., 2006; Grenz et al., 2011b), particularly through the ADORA2B (Eltzschig et al., 2013; Grenz et al., 2011b; Poth et al., 2013). Other studies had implicated the ADORA2B in cardioprotection from IR injury (Eckle et al., 2012; Eckle et al., 2007; Seo et al., 2015). To further investigate a potential role for ADORA2B signaling in netrin-1–dependent cardioprotection, we first conducted genetic studies in previously characterized mice with global deletion of the *Adora2b* (Fig. 4 A; Aherne et al., 2015; Seo et al., 2015). For this purpose, *Adora2b*$^{-/-}$ mice or WT control mice were subjected to 45 min of ischemia and 120 min of reperfusion. Recombinant murine netrin-1 (20 µg/kg) was given i.v. 5 min before reperfusion, while the control animals received an equal volume of PBS. A pilot study was first conducted in WT animals to determine the optimal dosage of netrin-1 (Fig. S4 A). Netrin-1 treatment significantly reduced myocardial IR injury in WT mice but was completely ineffective in reducing myocardial infarct sizes in *Adora2b*$^{-/-}$ mice (Fig. 4, B–D). Besides, 5 min before reperfusion, we additionally treated

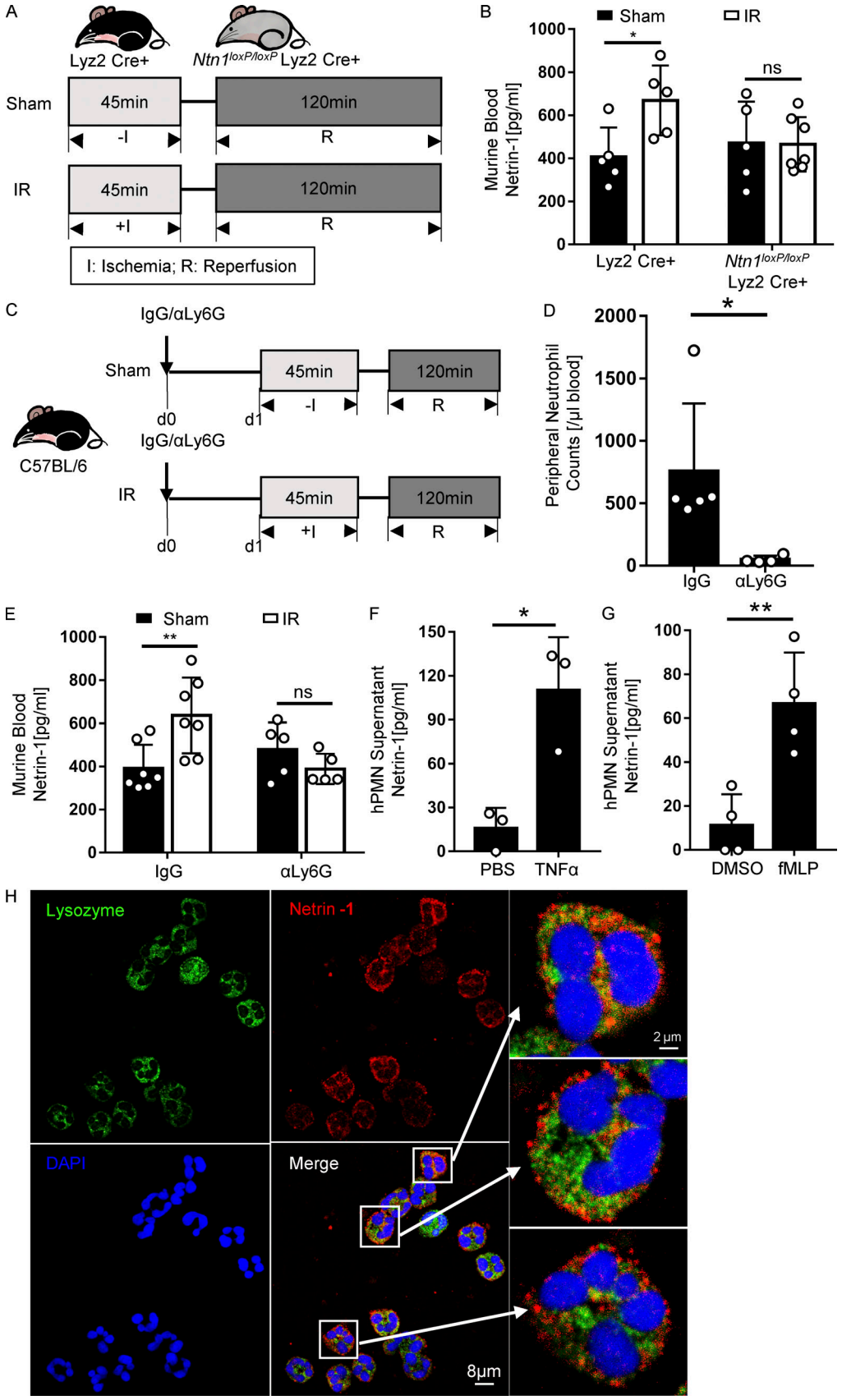

Figure 3. **Neutrophils release netrin-1 in response to murine cardiac IR injury and in vitro activation. (A and B)** Surgery strategy and blood netrin-1 levels of Lyz2 Cre$^+$ mice compared with *Ntn1*$^{loxP/loxP}$ Lyz2 Cre$^+$ mice after IR surgery (n = 5 for Lyz2 Cre$^+$, n = 5 and 7 for *Ntn1*$^{loxP/loxP}$ Lyz2 Cre$^+$ sham and IR

groups, respectively; two-way ANOVA with Bonferroni post hoc tests). **(C)** Neutrophil depletion and IR surgery strategy (IgG, IgG isotype control group; αLy6G, neutrophil depletion group). **(D)** Murine blood neutrophil cell counts after neutrophil depletion (n = 5 for isotype IgG control, n = 4 for αLy6G neutrophil depletion group; Mann-Whitney test). **(E)** Blood netrin-1 levels of WT (C57BL/6) mice with neutrophil depletion or IgG control after IR surgery (n = 7 for isotype IgG control, n = 5 for αLy6G neutrophil depletion group; two-way ANOVA with Bonferroni post hoc tests). **(F and G)** Netrin-1 level changes in supernatants of human PMN (hPMN) after being activated with TNFα or fMLP for 2 h; PBS or DMSO was used as a control, respectively (TNFα and PBS groups, data from three independent experiments; fMLP and DMSO groups, data from four independent experiments; two-tailed unpaired t test). **(H)** Immunofluorescence costaining of netrin-1 with lysozyme in human PMN shows that netrin-1 locates in the cytosol but not in the neutrophil lysozyme-containing granules. (For left four pictures, scale bar = 8 µm; for enlarged three pictures on the right, scale bar = 2 µm.) *, P < 0.05; **, P < 0.01. Data are presented as mean ± SD.

mice at the onset of ischemia (45 min before reperfusion) and also 20 min after ischemia (25 min before reperfusion) to see if the effectiveness is dependent on the time of treatment. Results of the infarct sizes of troponin levels showed protective effects of all three treatment time points (Fig. S4, B and C). Considering the clinical relevance, we chose to give netrin-1 five min before reperfusion for all subsequent experiments. As a second step, we implemented a pharmacologic approach by using PSB1115 (10 mg/kg) as a highly specific ADORA2B receptor antagonist (Eckle et al., 2008a) 20 min before ischemia (Fig. 4 E). Exogenous netrin-1 was given before reperfusion, as described above, and significant reduction of injury was observed in the control group. In contrast, PSB1115 treatment abolished the above-described cardioprotective effects of treatment with recombinant netrin-1 (Fig. 4, F–H). To address if netrin-1 directly induces adenosine, which could trigger downstream signaling events through the ADORA2B, we injected mice with recombinant netrin-1 (20 µg/kg) and measured adenosine levels in the serum and cardiac tissue samples 5 min, 25 min, and 45 min after netrin-1 treatment via HPLC. The findings demonstrate that adenosine levels in cardiac tissue or serum were not elevated following treatment with recombinant netrin-1 (Fig. S4, D and E). Collectively, these experiments indicate purinergic signaling events through the ADORA2B in mediating netrin-1–dependent cardioprotection from IR.

Myeloid-expressed ADORA2B is critical in mediating netrin-1–dependent cardioprotection

After having shown that purinergic signaling events through the ADORA2B are critical in mediating cardioprotection of netrin-1, we next pursued studies to address the tissue-specific roles for ADORA2B signaling. For this purpose, we exposed transgenic mice with tissue-specific *Adora2b* deficiency to myocardial IR injury in the presence or absence of recombinant netrin-1 treatment (Fig. 5 A). We used previously described mice with deletion of the *Adora2b* on vascular endothelia (*Adora2b*$^{loxP/loxP}$ VE-cadherin Cre^{+}; Hoegl et al., 2015), on cardiac myocytes (*Adora2b*$^{loxP/loxP}$ Myosin Cre^{+}; Seo et al., 2015), or on the myeloid compartment (*Adora2b*$^{loxP/loxP}$ Lyz2 Cre^{+}; Seo et al., 2015). Cre^{+} mice matched in age, weight, and sex for each generated strain were used as control animals. Recombinant mouse netrin-1 (20 µg/kg) was given i.v. 5 min before reperfusion, while the control animals received equal volumes of PBS. Significant reduction of myocardial injury was observed in netrin-1–treated *Adora2b*$^{loxP/loxP}$ VE-cadherin Cre^{+} or *Adora2b*$^{loxP/loxP}$ Myosin Cre^{+} mice, but not in *Adora2b*$^{loxP/loxP}$ Lyz2 Cre^{+} mice (Fig. 5, B–J). Based on these results, we conclude an important contribution of ADORA2B signaling in myeloid cells mediating myocardial protective effects of netrin-1 during myocardial IR injury.

Netrin-1 regulates neutrophil infiltration during myocardial IR via ADORA2B signaling

To further elucidate the impact of netrin-1 and myeloid ADORA2B signaling in neutrophil trafficking during myocardial reperfusion, we performed neutrophil transmigration assays using recombinant netrin-1–treated neutrophils in the presence or absence of PSB1115 (Fig. S5, A–C). Consistent with previous studies (Aherne et al., 2012; Mirakaj et al., 2010; Rosenberger et al., 2009), we demonstrate that netrin-1 attenuates neutrophil transmigration in vitro in an ADORA2B-dependent manner. To confirm that neutrophil migration is regulated by ADORA2B signaling in vivo, we used flow cytometry to determine the percentage of infiltrating neutrophils in digested *Adora2b*$^{loxP/loxP}$ Lyz2 Cre^{+} or Lyz2 Cre^{+} cardiac tissues after IR surgery with or without netrin-1 treatment (Fig. 6 A). Our data demonstrate that the fraction of neutrophils recruited into the myocardium increases significantly after IR surgery. Importantly, in Lyz2 Cre^{+} mice treated with recombinant netrin-1, we observed a significant reduction of infiltrating PMNs (Fig. 6, B and C). In contrast, and similar to the above in vitro studies, netrin-1 treatment failed to reduce infiltration of neutrophils into the myocardium of *Adora2b*$^{loxP/loxP}$ Lyz2 Cre^{+} mice (Fig. 6, D and E). Taken together, these findings indicate that treatment with recombinant netrin-1 decreases neutrophil transmigration in vitro or infiltration of neutrophils during myocardial IR in vivo in an ADORA2B–dependent manner, which may provide the pathophysiological basis for dampened tissue IR injury.

Discussion

Previous studies have implicated the neuronal guidance molecule netrin-1 in cardioprotection from IR injury (Mao et al., 2014; Ramesh et al., 2010; Siu et al., 2015; Zhang and Cai, 2010). However, the tissue-specific roles and detailed signaling events mediating its protective effects from IR injury remain less well defined. To make progress on this front, we performed studies of myocardial IR injury using mice with tissue-specific deletions of netrin-1. Using a previously described murine model of in situ myocardial IR injury (Eckle et al., 2006; Eckle et al., 2012; Koeppen et al., 2018; Lee et al., 2020), we found evidence that elevations of circulating levels of netrin-1 are predominantly PMN dependent. In addition, mice with deletion of netrin-1 in the myeloid compartment (*Ntn1*$^{loxP/loxP}$ Lyz2 Cre^{+} mice) experienced increased myocardial infarct sizes following IR injury. Based on previous studies indicating that netrin-1 interaction with the ADORA2B for extracellular adenosine plays a functional role in attenuating hypoxia-driven inflammation (Aherne et al., 2012; Duan et al., 2020; Mirakaj et al., 2011; Mirakaj et al., 2010;

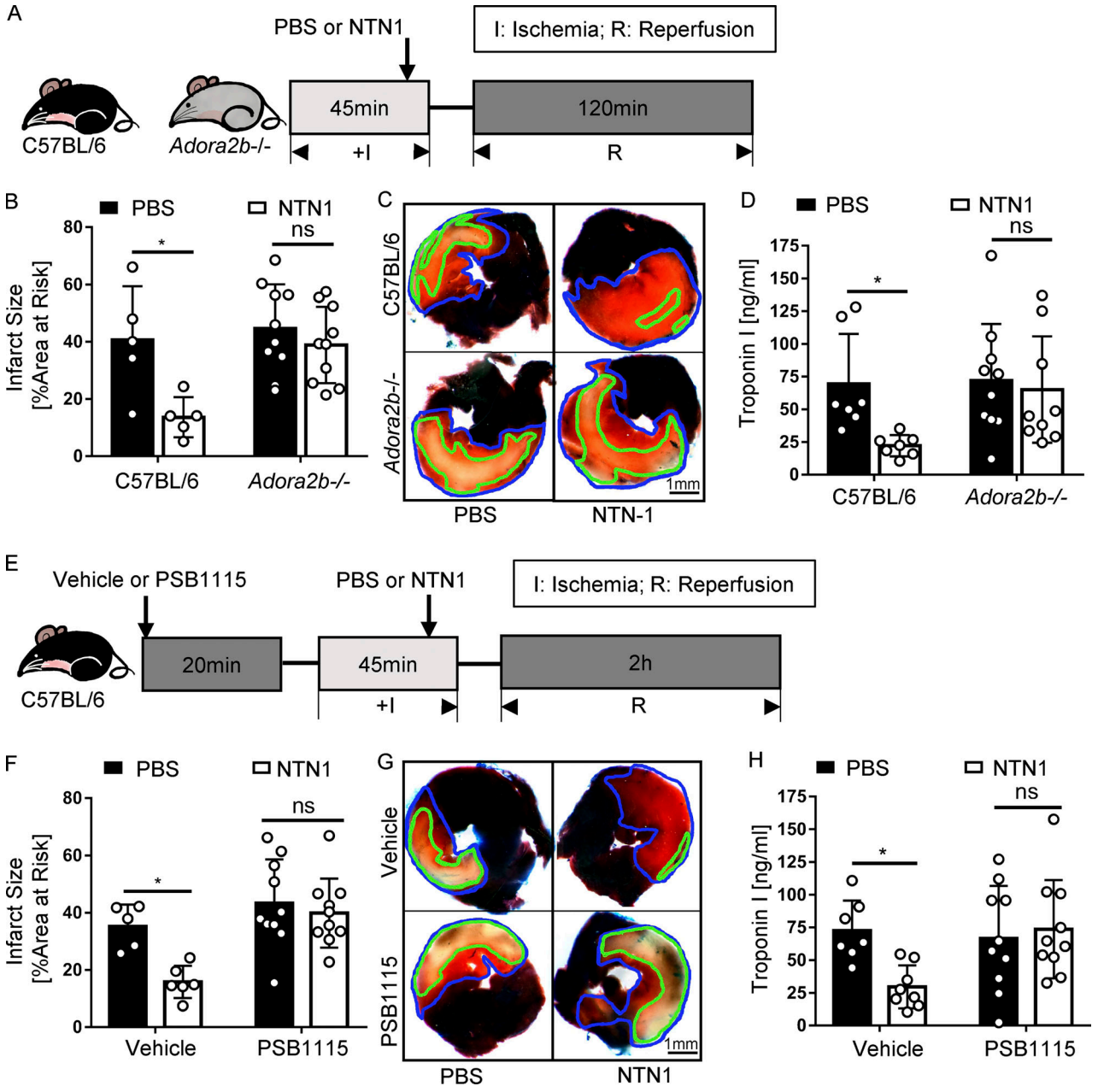

Figure 4. **Cardioprotection of netrin-1 is ADORA2B dependent. (A)** Surgery and netrin-1 treatment strategy. Recombinant mouse netrin-1 or PBS was given i.v. 5 min before reperfusion. **(B)** Infarct sizes of *Adora2b*$^{-/-}$ mice compared with WT mice after IR surgery with NTN1 treatment or PBS control (n = 10 for *Adora2b*$^{-/-}$ groups, n = 5 for WT groups; two-way ANOVA with Bonferroni post hoc tests). **(C)** Representative infarct staining results of *Adora2b*$^{-/-}$ mice and WT mice. The infarct area is outlined by a green line, and the blue line marks the AAR (scale bar = 1 mm). **(D)** cTnI levels of *Adora2b*$^{-/-}$ mice compared with WT mice after surgery and netrin-1 treatment (n = 10 for *Adora2b*$^{-/-}$ group, n = 7 for WT group; two-way ANOVA with Bonferroni post hoc tests). **(E)** ADORA2B receptor antagonist PSB1115 and netrin-1 treatment strategy. Recombinant mouse netrin-1 or PBS was given i.v. 5 min before reperfusion. **(F)** Infarct sizes of PSB1115-treated mice compared with vehicle control group after IR surgery with or without netrin-1 treatment (n = 10 for PSB1115-treated group, n = 5 and 6 for vehicle control group; two-way ANOVA with Bonferroni post hoc tests). **(G)** Representative infarct staining results of PSB1115-treated group and vehicle group. The infarct area is outlined by a green line, and the blue line marks the AAR (scale bar = 1 mm). **(H)** cTnI levels of PSB1115-treated mice compared with vehicle control mice after surgery and netrin-1 treatment (n = 10 for PSB1115-treated group, n = 7 and 8 for vehicle control group; two-way ANOVA with Bonferroni post hoc tests). *, P < 0.05. Data are presented as mean ± SD.

Schlegel et al., 2016; Zhang et al., 2018), we pursued the functional role of ADORA2B as a mediator of netrin-1–mediated cardioprotection. While we found that treatment with recombinant netrin-1 was associated with smaller infarct sizes and decreased troponin leakage in WT mice, these effects were abolished by PSB1115, a highly specific ADORA2B inhibitor (Eckle et al., 2008b). Similarly, we found that mice with global or myeloid deletion of the ADORA2B failed to be responsive to the cardioprotective effects elicited by treatment with recombinant netrin-1. Taken together, our studies indicate an

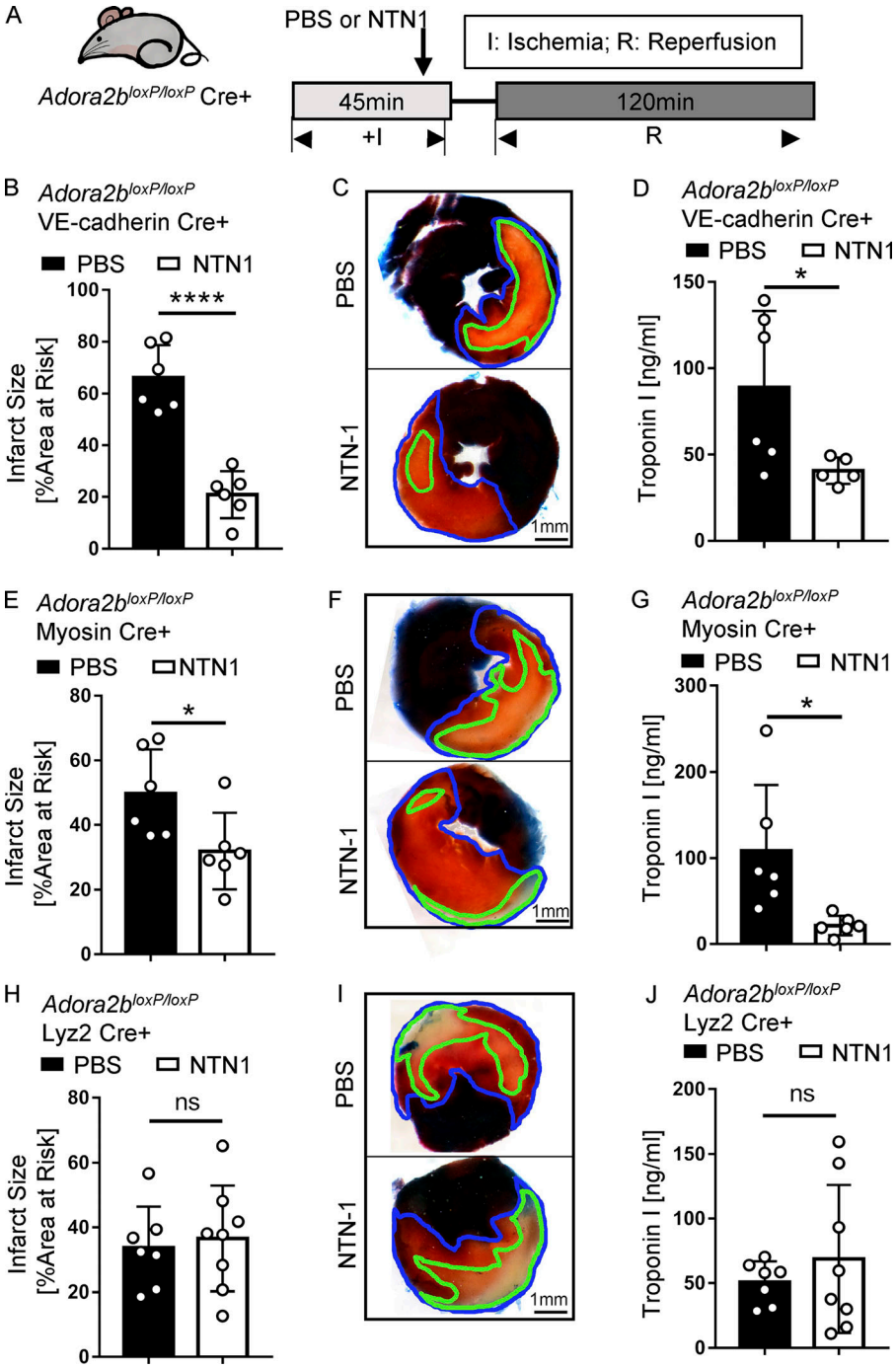

Figure 5. **Cardioprotection of netrin-1 is myeloid ADORA2B dependent. (A)** Surgery and netrin-1 treatment strategy. Recombinant mouse netrin-1 or PBS was given i.v. 5 min before reperfusion. **(B)** Infarct sizes of *Adora2b*$^{loxP/loxP}$ VE-cadherin Cre$^+$ mice compared with VE-cadherin Cre$^+$ mice (n = 6 per group; two-tailed unpaired t test). **(C, F, and I)** Representative infarct staining results of *Adora2b*$^{loxP/loxP}$ Cre$^+$ and corresponding Cre$^+$ mice. The infarct area is outlined by a green line, and the blue line marks the AAR (scale bar = 1 mm). **(D)** cTnI levels of *Adora2b*$^{loxP/loxP}$ VE-cadherin Cre$^+$ mice compared with VE-cadherin Cre$^+$ (n = 6 and 5 for PBS and netrin-1 treatment groups, respectively; two-tailed unpaired t test). **(E)** Infarct sizes of *Adora2b*$^{loxP/loxP}$ Myosin Cre$^+$ mice compared with Myosin Cre$^+$ mice (n = 6 per group; two-tailed unpaired t test). **(G)** cTnI levels of *Adora2b*$^{loxP/loxP}$ Myosin Cre$^+$ mice compared with Myosin Cre$^+$ (n = 6 per group; two-tailed Welch's t test). **(H)** Infarct sizes of *Adora2b*$^{loxP/loxP}$ Lyz2 Cre$^+$ mice compared with Lyz2 Cre$^+$ mice (n = 7 and 8 for PBS and netrin-1 treatment groups, respectively; two-tailed unpaired t test). **(J)** cTnI levels of *Adora2b*$^{loxP/loxP}$ Lyz2 Cre$^+$ mice compared with Lyz2 Cre$^+$ (n = 7 and 8 for PBS and netrin-1 treatment groups, respectively; two-tailed unpaired t test). ****, P < 0.0001; *, P < 0.05. Data are presented as mean ± SD.

autocrine signaling loop, with PMN-dependent netrin-1 released by PMNs and activation of myeloid expressed ADORA2B in mediating the cardioprotection conferred by netrin-1.

Netrin-1 was originally identified as a diffusible axon outgrowth-promoting protein in *Caenorhabditis elegans* (Serafini et al., 1994). Subsequent studies identified its role as a neuronal guidance molecule made by floor plate cells critical for development of the central nervous system (Serafini et al., 1996). However, more recent studies demonstrated that its expression is much more ubiquitous than originally anticipated (Mirakaj and Rosenberger, 2017). For example, several studies found expression and functional roles of netrin-1 released from the vagus nerve (Mirakaj et al., 2014) or expression in the mucosal surface of the lungs (Mirakaj et al., 2010; Rosenberger et al., 2009) or the intestine (Aherne et al., 2013; Rosenberger et al., 2009), hepatocytes (Schlegel et al., 2016), or renal tubular epithelia (Ranganathan et al., 2013). Several studies have also demonstrated expression of netrin-1 in immune cells, including expression and function in macrophages (Hadi et al., 2018) or neutrophils (Berg et al., 2021).

Previous studies of hypoxic tissue injury primarily implicated epithelium-derived netrin-1 in attenuating hypoxia-driven inflammation of mice exposed to ambient hypoxia (8% oxygen over 4 h), revealing increased netrin-1 expressed on the colonic

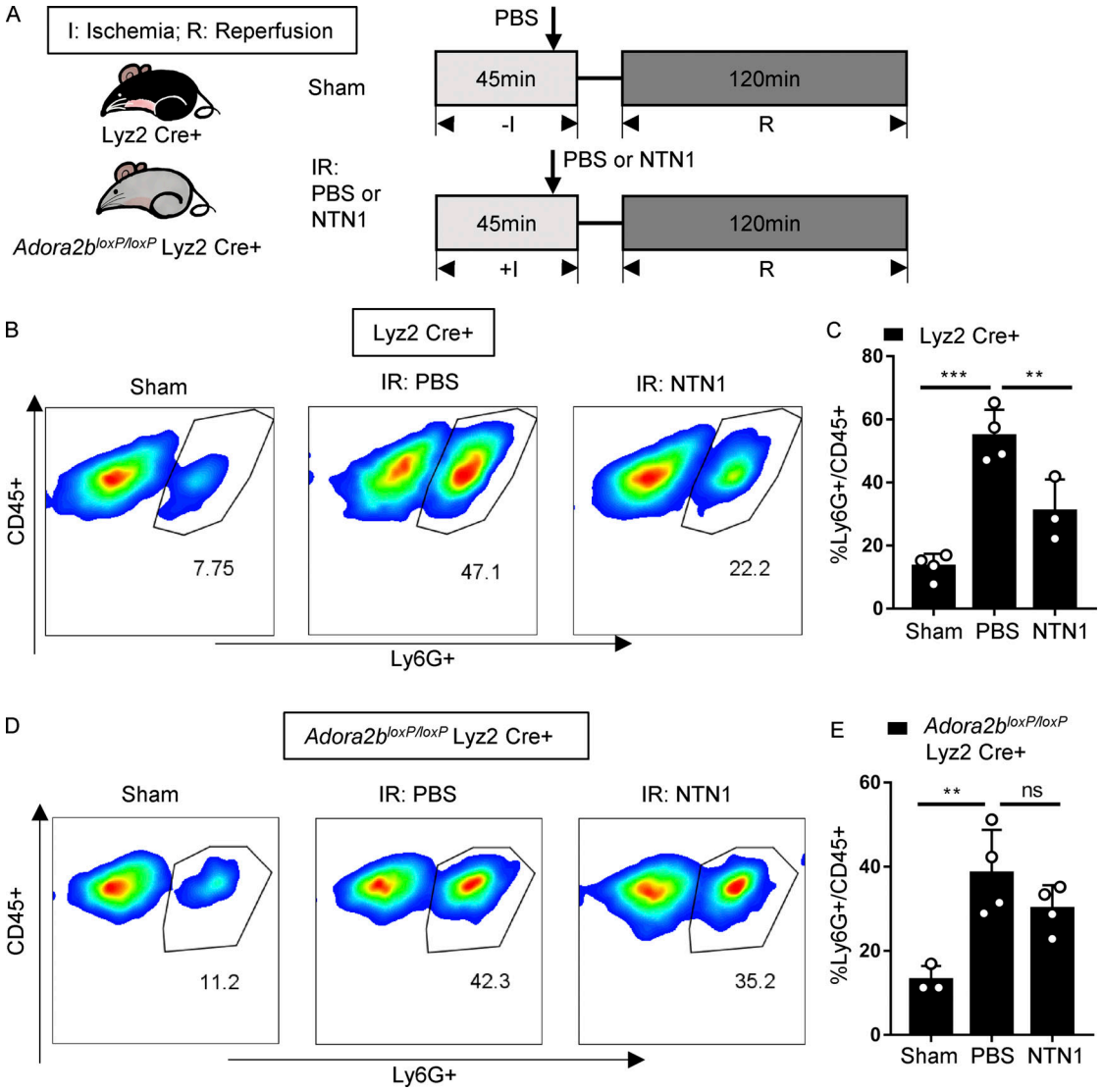

Figure 6. **Netrin-1 reduced neutrophil infiltration after cardiac IR is myeloid ADORA2B dependent. (A)** Surgery and netrin-1 treatment strategy. Recombinant mouse netrin-1 or PBS was given i.v. 5 min before reperfusion. **(B and C)** Neutrophil infiltration ($CD45^+Ly6G^+$) in Lyz2 Cre^+ mouse hearts after surgery was determined by flow cytometry (n = 4, 4, and 3 for sham group, PBS group, and NTN1 group, respectively; one-way ANOVA with Bonferroni post hoc tests). **(D and E)** Neutrophil infiltration ($CD45^+Ly6G^+$) in *Adora2b*$^{loxP/loxP}$ Lyz2 Cre^+ mouse hearts after surgery determined by flow cytometry (n = 3, 4, and 4 for sham group, PBS group, and netrin-1 group, respectively; one-way ANOVA with Bonferroni post hoc tests). **, $P < 0.01$; ***, $P < 0.001$. Data are presented as mean ± SD.

or lung epithelial cells (Rosenberger et al., 2009). Similarly, studies on the functional role of netrin-1 during intestinal inflammation in a murine model of inflammatory bowel disease showed elevated levels of netrin-1 in the mucosal lining of the inflamed colon (Aherne et al., 2013). A study by Mirakaj et al. showed that local expression of netrin-1 can be controlled by the vagus nerve and that vagotomy reduced local proresolving mediators, thereby delaying the resolution of inflammation (Mirakaj et al., 2014). Additionally, netrin-1 expressed in myeloid cells has also been described. For example, targeted deletion of netrin-1 in macrophages resulted in reduced atherosclerosis in mice deficient in the receptor for low-density lipoprotein and promoted the emigration of macrophages from plaques (van Gils et al., 2012), and the deletion of netrin-1 in macrophages protected mice from developing abdominal aortic aneurysms (Hadi et al., 2018). Here, our studies implicate neutrophil-derived netrin-1 as a major source for endogenous netrin-1 mediating the cardioprotective effects.

Consistent with our findings, previous studies have shown cardioprotective roles of netrin-1 during myocardial IR injury (Layne et al., 2015). These studies indicate an interaction of netrin-1 with its receptor DCC expressed on endothelial cells and myocytes, leading to ERK1/2/endothelial nitric oxide synthase phosphorylation and increased production of nitric oxide (Siu et al., 2015; Zhang and Cai, 2010). Other studies suggest that the expression of the E3 ubiquitin ligase seven in absentia homologue that is specific for regulation of proteasome-dependent DCC degradation plays a functional role in controlling the role

of netrin-1 and DCC-dependent cardioprotection (Li et al., 2015). In contrast to DCC, previous studies have suggested a detrimental role of the netrin-1 receptor UNC5 homologue B during myocardial IR injury (Köhler et al., 2013). In contrast, our findings suggest ADORA2B signaling on myeloid cells in mediating cardioprotection by netrin-1. It has been shown previously that the signal transduction of netrin-1 requires interaction with ADORA2B to mediate anti-inflammatory protection by regulating neutrophil migration and infiltration, for example during acute lung injury (Mirakaj et al., 2010), diabetic corneal injury (Zhang et al., 2018), inflammatory bowel disease (Aherne et al., 2012), and liver IR injury (Schlegel et al., 2016). The mechanism by which netrin-1 enhances ADORA2B signaling during cardioprotection from IR remains unclear. It is conceivable that netrin-1 stimulates the release of adenosine in cardiac tissues, which in turn activates the ADORA2B on PMNs. For example, this could be explained by a functional role of netrin-1 in inhibiting adenosine transporters (Eckle et al., 2013) or adenosine metabolism (Morote-Garcia et al., 2008). In contrast, the present studies of adenosine measurements in the serum or cardiac tissues indicate that adenosine levels are unaltered following treatment with recombinant netrin-1 (Fig. S4, D and E). While it is possible that netrin-1 could function as a direct ligand of the ADORA2B, netrin-1 could also bind a classical netrin-1 receptor (e.g., DCC or UNC5 homologue), resulting in enhancement of ADORA2B signaling, e.g., by enhancing signal transduction events. Nevertheless, the current findings support a link between netrin-1 and adenosine signaling through ADORA2B in attenuating tissue inflammation that occurs during conditions of limited oxygen availability, such as during myocardial IR injury.

It is well established that extracellular adenosine signaling events attenuate inflammation (Eltzschig et al., 2012; Haskó and Cronstein, 2004; Haskó et al., 2009; Haskó et al., 2008; Ohta and Sitkovsky, 2001) or protect the myocardium from IR injury (Eltzschig et al., 2013; Poth et al., 2013). During myocardial injury, many cells release nucleotides, such as ATP and ADP, that serve as the metabolites for the generation of adenosine. Mice with genetic deletion of the enzymatic control for extracellular generation from precursor nucleotides show elevated myocardial infarct sizes (Eckle et al., 2007; Köhler et al., 2007). Different adenosine receptors have been implicated as regulators of cardiac physiology (Koeppen et al., 2009) and cardioprotection (Eckle et al., 2012; Eckle et al., 2008c; Matherne et al., 1997; Seo et al., 2015). Adenosine can signal through four different adenosine receptors (ADORA1, ADORA2A, ADORA2B, and ADORA3; Idzko et al., 2014; Poth et al., 2013). A head-to-head comparison of mice with global deletion of each individual adenosine receptor specifically implicated ADORA2B in mediating the cardioprotection conferred by ischemic preconditioning (Eckle et al., 2007). Subsequent studies addressing tissue-specific functions of ADORA2B signaling during myocardial IR injury revealed important protection of myeloid-dependent ADORA2B signaling (Seo et al., 2015). These findings are consistent with our studies showing that netrin-1–dependent cardioprotection involves myeloid ADORA2B signaling events.

Previous studies have linked the expression of netrin-1 with transcriptional responses through the hypoxia-inducible transcription factor HIF1A (Ramkhelawon et al., 2013; Rosenberger et al., 2009). This transcription factor was discovered in the early 1990s (Wang et al., 1995; Wang and Semenza, 1993). Consistent with a functional role of hypoxia inducible factor (HIF) in cardioprotection, mice with heterozygous deletion of *Hif1a* are not protected by ischemic preconditioning, an experimental strategy that is associated with attenuated myocardial infarct sizes (Cai et al., 2008; Semenza, 2011). Similarly, studies directly implicate HIF1A in remote ischemic preconditioning of the heart, where remote ischemia provides robust cardioprotection through induction of the HIF target gene IL-10 (Cai et al., 2013). Other studies have linked the anti-inflammatory and tissue-protective roles of HIF to adenosine signaling, particularly through the ADORA2A and ADORA2B (Ohta and Sitkovsky, 2001; Sitkovsky et al., 2004; Thiel et al., 2005). For example, studies highlight that many tissue-protective responses of HIF are mediated through the activation of adenosine receptors (Sitkovsky and Lukashev, 2005; Sitkovsky et al., 2004). In line with these studies, mice with siRNA-mediated HIF inhibition experience larger infarct size due to attenuated ADORA2B signaling (Eckle et al., 2008c; Eltzschig et al., 2013). Since the expression of netrin is directly regulated by HIF in myeloid cells (Ramkhelawon et al., 2013; Rosenberger et al., 2009), it seems likely that HIF1A could play a functional role in coordinating netrin-1–dependent cardioprotection during IR injury of the heart.

The present studies suggest that PMNs function as an important source for netrin-1 liberation during myocardial IR injury. Several previous studies have investigated mechanisms by which neutrophils can be activated during myocardial IR injury, leading to the release of inflammatory or anti-inflammatory mediators, such as netrin-1 (Hansen, 1995). Activation of PMNs during myocardial injury can occur during their interaction with endothelia or their interaction with injured myocytes, such as the myocyte-dependent expression of intercellular adhesion molecule ICAM-1 (Smith et al., 1991). Moreover, infarcted myocardium, the death of cardiomyocytes, and the concomitant degradation of extracellular matrix components that are being released have been shown to activate innate immune cells, including neutrophils (Frangogiannis, 2014; Yellon and Hausenloy, 2007). Neutrophils, which represent the largest population of circulating leukocytes in the human body (50–70%; Kolaczkowska and Kubes, 2013), were thought to be detrimental during MI for decades due to their early infiltration into the infarcted myocardium. Neutrophils may cause a no-reflow phenomenon and generate ROS along with degranulation that release a massive number of proteases and proinflammatory factors and consequently cause excessive tissue injury, especially in the ischemic border zone (Hansen, 1995; Vinten-Johansen, 2004). Therefore, various antineutrophil therapies have been attempted in the past 20 yr, including leukocyte depletion and protease inhibitors (Puhl and Steffens, 2019). However, there are controversial opinions against the detrimental involvement of neutrophils in the myocardial IR injury (Silvestre-Roig et al., 2020), and antineutrophil clinical studies have shown negative results (Vinten-Johansen, 2004), indicating that neutrophils may be essential to contain the IR injury during MI. Our studies here show the regulation of

neutrophil infiltration by neutrophil-derived netrin-1 during IR, which provides insight into the emerging role of neutrophils during cardioprotection. Since neutrophils also serve as the main tissue-specific source for the release of netrin-1, this could be interpreted as an autocrine stopping signal of self-limited neutrophil inflammation.

Several limitations of the current studies should be pointed out. It could be conceived that netrin-1 signaling functions to precondition or educate myeloid progenitors to be developmentally biased toward an anti-inflammatory impact. In fact, previous studies suggest that netrin-1 can have an impact by educating progenitor cells, for example on neural progenitor cells during axon guidance (Varadarajan et al., 2017). However, since the present studies demonstrate immediate signaling effects by treating mice with recombinant netrin, it appears more unlikely that the observed cardioprotection is related to preconditioning or education of myeloid progenitor cells. While the current studies are focused on functional roles of the signaling molecule netrin-1 during myocardial IR injury, other neuronal guidance molecules have been implicated in orchestrating inflammatory endpoints as well (Keller et al., 2021; Mirakaj and Rosenberger, 2017). For example, a recent study showed elegantly that RBC-derived semaphorin 7A promotes thromboinflammation in an in situ model of murine myocardial IR injury (Köhler et al., 2020). Other studies implicate neogenin (Schlegel et al., 2018) or repulsive guidance molecule RGM-A in orchestrating inflammatory endpoints (Körner et al., 2019). Moreover, other myeloid-derived signals have previously been shown to dampen IR injury. For example, neutrophils have been shown to release nucleotides upon activation through connexin hemichannels (Eltzschig et al., 2006; Eltzschig et al., 2008). Such nucleotides in this form can be converted rapidly to adenosine and function to activate ADORA2B and dampen myocardial IR injury (Eckle et al., 2007; Ferrari et al., 2016). Other studies demonstrated that neutrophils can release microvesicles that contain microRNAs, which in turn can dampen inflammatory responses of the surrounding tissues (Neudecker et al., 2017; Yuan et al., 2018). An additional limitation of the current studies relates to the fact that only a relatively short reperfusion time period was used (120 min), and it remains somewhat unclear if the protection afforded by PMN-derived netrin-1 would be sustained during a longer recovery process. However, previous studies by other investigators have shown that netrin-1 treatment provides cardioprotection using longer reperfusion time periods (e.g., 24 h) or in models of permanent coronary occlusion over 2 wk (Bouhidel et al., 2015), indicating the likelihood that the early protection observed in the present studies could be sustained with longer reperfusion periods.

In summary, our results demonstrate that neutrophil-derived netrin-1 provided cardioprotection from myocardial IR injury. Attenuating myocardial injury and decreased neutrophil trafficking into the myocardium is regulated through signaling events on myeloid-expressed ADORA2B. Together, these findings provide additional evidence for a cardioprotective function of netrin-1 by dampening myocardial reperfusion injury that could be targeted for the treatment of patients experiencing myocardial injury.

Materials and methods

MI patient and healthy donor samples

Serum/plasma samples of patients with MI or healthy donors were purchased from Discovery Life Sciences. Corresponding cTnI levels of patients with MI were documented in the patient sample data sheet. (The patient data sheet and healthy donor data sheet are shown in Table S1 and Table S2.)

Mice

All animal experiments and procedures were approved by the University of Texas Health Science Center at Houston Institutional Animal Care and Use Committee. Sex- and weight-matched mice aged between 8 and 16 wk were used. WT (C57BL/6J, JAX stock no. 000664), netrin-1 floxed (*Ntn1*$^{loxP/loxP}$, B6.129(SJL)-Ntn1tm1.1Tek/J, JAX stock no. 028038; Bin et al., 2015), CMV Cre$^+$ (B6.C-Tg(CMV Cre)1Cgn/J, JAX stock no. 006054; Schwenk et al., 1995), Lyz2 Cre$^+$ (B6.129P2-Lyz2tm1(cre)Ifo/J, JAX stock no. 004781; Clausen et al., 1999), VE-cadherin Cre$^+$ (B6.FVB-Tg(Cdh5 Cre)7Mlia/J, JAX stock no. 006137; Alva et al., 2006) and Myosin Cre$^+$ (A1cfTg(Myh6 Cre/Esr1*)1Jmk/J, JAX stock no. 005650; Sohal et al., 2001) mice were purchased from The Jackson Laboratory. *Adora2b* floxed (*Adora2b*$^{loxP/loxP}$) mice were generated by Ozgene (Seo et al., 2015). *Adora2b*$^{-/-}$ mice were generated by crossbreeding *Adora2b*$^{loxP/loxP}$ mice with CMV Cre$^+$ and WT mice were used as control. *Adora2b*$^{loxP/loxP}$ VE-cadherin Cre$^+$, *Adora2b*$^{loxP/loxP}$ Myosin Cre$^+$, *Adora2b*$^{loxP/loxP}$ Lyz2 Cre$^+$, *Ntn1*$^{loxP/loxP}$ Myosin Cre$^+$, and *Ntn1*$^{loxP/loxP}$ Lyz2 Cre$^+$ mice were obtained by crossbreeding floxed mice with corresponding Cre recombinase mice (Seo et al., 2015). To induce the Cre recombinase of Myosin Cre$^+$ mice, mice were subjected to tamoxifen diet (Envigo no. TD.130860) for 3 wk. Animals were genotyped to ensure Cre$^+$ and knock-down efficiencies were confirmed (Seo et al., 2015). Considering injury variations caused by animal backgrounds, Cre$^+$ littermates were used as control. To minimize animal usage, pilot experiments and power analysis were performed to determine the sample sizes (Koeppen et al., 2018; Lee et al., 2020).

Adora2b$^{-/-}$ mice and tissue-specific *Adora2b*-deficient mice

Adora2b$^{-/-}$ mice were generated by crossbreeding *Adora2b* floxed mice (Ozgene) with CMV Cre$^+$ to obtain whole-body knockout, and WT mice were used as control. *Adora2b*$^{loxP/loxP}$ VE-cadherin Cre$^+$, *Adora2b*$^{loxP/loxP}$ Myosin Cre$^+$, and *Adora2b*$^{loxP/loxP}$ Lyz2 Cre$^+$ mice were obtained by crossbreeding *Adora2b*$^{loxP/loxP}$ mice with VE-cadherin Cre$^+$, Myosin Cre$^+$, and Lyz2 Cre$^+$, respectively. To induce the Cre recombinase of Myosin Cre$^+$ mice, mice were subjected to tamoxifen diet for 3 wk. Tissue-specific deficient animals were genotyped to ensure Cre$^+$ and knock-down efficiencies were confirmed in our laboratory as described before (Seo et al., 2015). Cre$^+$ littermates were used as control.

Tissue-specific netrin-1–deficient mice

Ntn1$^{loxP/loxP}$ mice were crossbred with Myosin Cre$^+$ and Lyz2 Cre$^+$ respectively to generate *Ntn1*$^{loxP/loxP}$ Myosin Cre$^+$ and *Ntn1*$^{loxP/loxP}$ Lyz2 Cre$^+$ mice. To induce the Cre recombinase of Myosin Cre$^+$ mice, all mice were subjected to tamoxifen diet for 3 wk. Tissue-specific deficient animals were genotyped to ensure Cre$^+$ and knock-down efficiencies were confirmed (Fig. S3). Cre$^+$ mice were used as control.

Murine model for myocardial IR injury

As previously described by our group, in situ IR injury was induced by a hanging weight system (Eckle et al., 2011; Koeppen et al., 2018). Briefly, anesthesia was induced (70 mg/kg i.p.) and maintained (10 mg/kg/h i.p.) with pentobarbital sodium (McKesson; no. 809790). Mice were intubated and connected to a mechanical ventilator (Carefusion/VIASYS AVEA) during the surgery (with pressure control mode, frequency of 100 breaths/min, inspiratory pressure of 14 cm H_2O, positive end-expiratory pressure of 4 cm H_2O, and FiO_2 of 0.4). The body temperature was maintained at 37°C using a temperature-controlled heating pad. A catheter was placed into the carotid artery for fluid replacement, an 8-0 suture (Prolene, Ethicon) was placed around the LCA following left lateral thoracotomy, and Eppendorf tubes were applied as weights to each end of the suture (Lee et al., 2020). After 45 min of ischemia, the weights were removed and reperfusion was continued for 2 h. The sham surgery groups underwent a similar surgical procedure without applying the hanging weights.

Infarct size measurement

The infarct size was determined by the percentage of infarcted area relative to the area at risk (AAR) as described previously (Eckle et al., 2006). The heart was flushed via the carotid artery catheter at the end of reperfusion. Evans blue (Sigma-Aldrich, MKCB2532V; 1%) was injected through the carotid artery catheter following LCA total occlusion. The heart was excised and kept at −20°C for 15 min and then sliced into 1 mm sections using a heart matrix (Roboz). After incubation with 1% triphenyltetrazolium chloride (Sigma-Aldrich, BCBR5461) for 10 min at 37°C, heart slices were placed in 10% neutral-buffered formalin overnight and images were acquired with a Nikon D5300 digital camera mounted on an Olympus SZX10 microscope with ×32 magnification. The AAR was determined by Evan's blue stain free area while the infarction was indicated by the triphenyltetrazolium chloride stain-free parts using ImageJ software (National Institutes of Health).

Murine blood netrin-1 and cTnI ELISA

The serum was collected at the end of reperfusion and stored at −80°C for further use. Blood netrin-1 levels were measured with mouse netrin-1 ELISA kits (LSBio; catalog no. LS-F5882). Myocardial injury was evaluated by measuring cTnI levels via ELISA (Life Diagnostic; catalog no. CTNI-1-HS) following the manual, as we have done previously (Eckle et al., 2006; Seo et al., 2015).

Recombinant murine netrin-1 treatment

Recombinant murine netrin-1 was purchased from R&D Systems (catalog no. 1109-N1/CF). After reconstitution with PBS, 20 µg/kg netrin-1 protein was given to the netrin-1 treatment group 5 min before reperfusion via the right jugular vein. The PBS groups were given the equivalent PBS as a control.

PSB1115 treatment

Adenosine A2b receptor antagonist PSB1115 was purchased from R&D Systems and dissolved in PBS (pH adjusted to 7.4). As described before (He et al., 2014), 10 mg/kg PSB1115 was injected via the tail vein 20 min before ischemia. Vehicle groups were given the equivalent vehicle solution as a control.

Murine PMN depletion

24 h before surgery, a single dose of αLy6G (Ly6G-specific antibody, 1A8; Bio X Cell; catalog no. BP0075-1) was given to mice (1 mg i.p.) as described previously (Neudecker et al., 2017). The IgG group was given the equivalent mouse IgG1 isotype protein (Bio X Cell; catalog no. BE0083) as a control. Effective neutrophil depletion was confirmed in the peripheral blood by cytospin, and cell number was counted under a microscope.

Monocyte and macrophage depletion

Mice were given 100 µl/10 g body weight i.v. clodronate liposomes (Liposoma BV) 24 h before surgery to deplete monocytes and macrophages as described before (Neudecker et al., 2017). Control mice received liposomes only at the same time points.

Murine PMN infiltration analysis with flow cytometry

Hearts were harvested after surgery for digestion to isolate infiltrated PMNs. The digestion was modified from a protocol described before (Ackers-Johnson et al., 2016). Mice were euthanized and perfused through a carotid artery catheter with normal saline and EDTA buffer (130 mmol/liter NaCl, 5 mmol/liter KCl, 0.5 mmol/liter NaH_2PO_4, 10 mmol/liter Hepes, 10 mmol/liter glucose, 10 mmol/liter 2,3-butanedione monoxime [BDM], 10 mmol/liter taurine, and 5 mmol/liter EDTA, pH 7.8) at the end of reperfusion, and the hearts were excised with atria and right ventricles removed (AAR is limited in the left ventricle). Then the left ventricles were minced into pieces by blades and mixed with collagenase buffer (130 mmol/liter NaCl, 5 mmol/liter KCl, 0.5 mmol/liter NaH_2PO_4, 10 mmol/liter Hepes, 10 mmol/liter glucose, 10 mmol/liter BDM, 10 mmol/liter taurine, 1 mmol/liter $MgCl_2$, 0.5 mg/ml collagenase II, 0.5 mg/ml collagenase IV, 0.05 mg/ml protease XIV, pH 7.8). The following digestion step was performed with gentleMACS Octo Dissociator with Heaters (Miltenyi Biotec) using the protocol 37 multi-G. After the digestion, the cell suspension was passed through a 100-µm strainer and pelleted with centrifugation. Cells were suspended in the gradient buffer (HBSS[−], 25 mM Hepes, 1 mM EDTA) and loaded on top of a density gradient cell separation medium (Histopaque-1119; Sigma-Aldrich). After centrifugation at 700 ×*g* for 30 min at room temperature without break, cells that remained in the interface were collected and stained with CD45-conjugated (clone 30-F11; BioLegend) and Ly6G-conjugated (clone 1A8; BioLegend) antibodies. Flow cytometry was performed with CytoFLEX LX (Beckman Coulter), and FlowJo version 10 (FlowJo LLC) was used to analyze data.

Murine PMN isolation

Murine PMNs were isolated from the bone marrow using the EasySep Mouse Neutrophil Enrichment Kit (STEMCELL Technologies) according to the manual. Briefly, the bone marrow was harvested from femurs and tibias after mice were euthanized. PMNs were negatively selected in an EasySep Magnet after the biotinylated antibody cocktail and EasySep D magnetic particle incubation.

Adult murine cardiomyocyte isolation

Briefly, mouse hearts were harvested following perfusion through the carotid artery catheter with normal saline and EDTA buffer (130 mmol/liter NaCl, 5 mmol/liter KCl, 0.5 mmol/liter NaH_2PO_4, 10 mmol/liter Hepes, 10 mmol/liter glucose, 10 mmol/liter BDM, 10 mmol/liter taurine, and 5 mmol/liter EDTA) after euthanization. Then the hearts were minced into pieces by blades and mixed with collagenase buffer (130 mmol/liter NaCl, 5 mmol/liter KCl, 0.5 mmol/liter NaH_2PO_4, 10 mmol/liter Hepes, 10 mmol/liter glucose, 10 mmol/liter BDM, 10 mmol/liter taurine, 1 mmol/liter $MgCl_2$, 0.5 mg/ml collagenase II, 0.5 mg/ml collagenase IV, 0.05 mg/ml protease XIV, pH 7.8). The following dissociation step was performed with gentleMACS Octo Dissociator with Heaters (Miltenyi Biotec) using protocol 37 multi-G. After the digestion, the cell suspension was passed through a 100-µm strainer, and the cardiomyocytes were collected as described before (Ackers-Johnson et al., 2016).

Murine serum and tissue adenosine measurement

Serum and heart tissue adenosine levels were measured as described previously (Eckle et al., 2013; Wakamiya et al., 1995). In brief, serum samples were mixed with inhibitor cocktail (10 µM dipyridamole; Sigma-Aldrich; catalog no. D9766), 10 µM deoxycoformycin (adenosine deaminase inhibitor; R&D Systems; catalog no. 2033), and 10 µM αβ-methylene ADP (Sigma-Aldrich; catalog no. M3763) to preserve nucleosides. Hearts were pulverized with liquid nitrogen immediately after harvest and homogenized in PBS on ice with protease inhibitor cocktail added. The supernatant was collected after centrifugation and protein concentrations were measured. Nucleosides were extracted by using perchloric acid and neutralized with $KHCO_3$/KOH. Samples were acidified with ammonium dihydrogen phosphate and phosphoric acid, and supernatant was collected after centrifugation. To measure adenosine levels, samples were analyzed by reverse-phase HPLC. Representative peaks were identified and quantified using external standard curves.

Human PMN isolation

The protocol was approved by the University of Texas Health Science Center at Houston Institutional Review Board to collect and use human PMNs from healthy volunteers, and written informed consent was signed by each individual before the blood draw. 50 ml of blood was obtained by venipuncture and anticoagulated with 10 ml of acid-citrate-dextrose buffer (Sigma-Aldrich; catalog no. C3821). After centrifugation at 400 ×*g* for 10 min at 4°C, the plasma was centrifuged at 400 ×*g* for another 10 min to pellet cells for a higher PMN yield. The cell pellet was added back to the remaining blood. The blood was mixed with 15 ml of 3% dextran (Sigma-Aldrich; catalog no. 31392) normal saline solution for sedimentation. The first phase was collected after sedimentation, and cells were pelleted after centrifugation at 400 ×*g* for 10 min at 4°C. The cell pellet was suspended in RBC lysis buffer (Miltenyi Biotec; catalog no. 130-094-183) to remove the remaining RBCs. After centrifugation, cells were suspended in gradient buffer (HBSS[−], 25 mM Hepes, 1 mM EDTA) and loaded carefully on top of the density gradient cell separation medium (Histopaque-1077; Sigma-Aldrich). After centrifugation at 700 ×*g* for 30 min at 4°C without break, supernatant was removed. PMNs containing pellet were washed twice in precold washing buffer (HBSS[−], 25 mM Hepes, 10% heat-inactivated FBS). The viability of the cells after isolation was >97% using the trypan blue dye exclusion test, and the purity was >95% as confirmed by using cytospin and the Hema3 Staining Pack (Fisher Diagnostics).

Human PMN activation

For activation, PMNs were suspended in RPMI 1640 medium at a density of 5 million/ml supplemented with 20 ng/ml TNFα or 100 nM fMLP and incubated at 37°C for 2 h, 4 h, and 6 h. After incubation, cells were pelleted by centrifugation at 1,000 ×*g* for 10 min, and both supernatant and pellets were kept at −80°C immediately.

PMN transmigration assay

6.5-mm Transwell inserts with 8.0-µm pores (Corning) were coated with 200 µg/ml extracellular matrix gel (Sigma-Aldrich; catalog no. E1270) and incubated at 37°C for 1 h. Human or murine PMNs were suspended in RPMI 1640 medium containing 1% heat-inactivated FBS at a density of 4 million/ml. For inhibition of adenosine A2b receptor, PMNs were incubated with 20 µM PSB1115 for 30 min. To study the effects of netrin-1, PMNs were incubated with 500 ng/ml recombinant mouse or human netrin-1 (R&D Systems) for 30 min before being loaded into inserts (0.2 million PMNs per insert). The lower chambers of Transwells were filled with 500 µl RPMI 1640 medium containing 1% heat-inactivated FBS and 100 nM fMLP. Cell numbers in the lower chambers were counted after 1 h.

Human blood netrin-1 ELISA

Human netrin-1 ELISA kits (LSBio; catalog no. LS-F5003) were used to measure the netrin-1 levels of human blood samples and activated human neutrophil supernatant according to the manual instructions.

Transcriptional analysis

Total RNA was isolated from the mouse tissue and human PMNs using TRIzol reagent according to the manufacturer's instructions (QIAzol Lysis Reagent; Qiagen; catalog no. 79306). Mouse tissue was snap frozen in liquid nitrogen after harvest, kept in a −80°C freezer, and homogenized in lysis reagent upon RNA isolation. Human PMNs were lysed in the lysis reagent and kept in a −80°C freezer until use. After chloroform was added, samples were spun at 12,000 ×*g* for 20 min, the first phase was collected, and the RNA was precipitated with the isopropanol method. The precipitated RNA was pelleted, washed twice with 70% ethanol, and dissolved in diethylpyrocarbonate-treated water, and the concentration was quantified with the BioTek Cytation 5 reader. cDNA synthesis was performed by using the Applied Biosystems High-Capacity Reverse Transcription Kit (Thermo Fisher Scientific; catalog no. 4368814) on the Bio-Rad T100 cycler. The real-time PCR reactions containing 1 µM sense and 1 µM antisense oligonucleotides with SYBR Green (QuantiTect SYBR Green PCR Kit; Qiagen; catalog no. 204145) were performed on the Bio-Rad CFX384 Touch Real-Time PCR

Detection System according to the QuantiTect SYBR Green protocol. Primer sets (reverse/ forward): NTN-1: 5′-AGGCAG ACACCTCCGCTCTT/CGAGTGCGTGGCCTGTAAC-3′; ACTB: 5′-ACTGGAACGGTGAAGGTGACAG/GGTGGCTTTTAGGATGGC AAG-3′; ADORA2B: 5′-CCGTGACCAAACTTTTATACCTG/GGG CTTCTGCACTGACTTCT-3′; Ntn-1: 5′-TGGTTTGATTGCAGGTCT TG/GAGCGGGGGAGTCTGTCT-3′; Actb: 5′-TCTGCTGGAAGG TGGACAG/GGCTCCTAGCACCATGAAGA-3′; Adora2b: 5′-GTG GGGGTCTGTAATGCACT/AGCTAGAGACGCAAGACGC-3′.

Immunoblotting experiments

Protein samples were prepared from cell pellets or murine heart samples with radioimmunoprecipitation assay buffer (20 mM Hepes, pH 7.4, 100 mM NaCl, 1 mM EDTA, 1% Triton X-100, 5% glycerol). After the abstraction, protein samples were solubilized in reducing Laemmli sample buffer and heated to 95°C for 5 min. The electrophoreses were performed with the Bio-Rad Mini-PROTEAN Tetra System and transferred to nitrocellulose membranes (Trans-Blot Turbo; Bio-Rad Laboratories). The membranes were blocked for 60 min at room temperature in PBS with Tween 20 (PBS-T) supplemented with 5% skim milk. Primary and secondary antibodies used for detection were as follows: netrin-1 antibody (ab126729, 1:1,000; Abcam), GAPDH antibody (97166, 1:2,000; Cell Signaling Technology), β-actin (sc-47778, 1:2,000; Santa Cruz Biotechnology), anti-rabbit (7074, 1:5,000; Cell Signaling Technology), and anti-mouse (7076, 1:5,000; Cell Signaling Technology). The membranes were incubated in 1:1,000 diluted primary antibodies at 4°C overnight, followed by three 15-min washes in PBS-T. Subsequently, membranes were incubated in 1:5,000 diluted secondary antibodies for 1 h at room temperature, followed by another series of three 15-min washes in PBS-T. Membranes were developed with enhanced chemiluminescence (SuperSignal West Femto Maximum Sensitivity Substrate; Thermo Fisher Scientific) by the Bio-Rad ChemiDoc Touch Imaging System. Stripped membranes were blotted for protein loading controls. Protein levels were quantified using ImageJ software (National Institutes of Health).

Immunohistochemistry

Hearts were fixed in neutral-buffered formalin and processed by Leica TP1020 processor followed by paraffin embedding by routine methods. The heart slices were cut in 4.5-µm sections and mounted on glass slides. Antigen retrieval was performed with citric acid–based antigen unmasking solution (Vector Laboratories; catalog no. H-3300) following deparaffinization and rehydration. After blocking with 2.5% normal goat serum (Vector Laboratories; catalog no. S-1000), slices were incubated with primary antibody (netrin-1 antibody, LS-C743016, 1:200; LifeSpan BioSciences) at 4°C overnight. The following steps were performed with the VECTASTAIN Elite ABC-HRP Kit (Vector Laboratories; catalog no. PK-6101) and the DAB Substrate Kit (Vector Laboratories; catalog no. SK-4100) according to the manual instructions, followed by hematoxylin counterstaining. Negative control slices were incubated with the recombinant rabbit IgG (Abcam; ab172730) instead of primary antibody at the same concentration. A Leica DM2500 light microscope was used to evaluate the staining, and pictures were taken with a Leica DMC5400 digital camera.

Immunofluorescence

Mouse hearts were harvested after surgery with 4% paraformaldehyde (PFA) perfused via a carotid artery catheter and fixed in 4% PFA for 0.5 h. After dehydration with sucrose, tissue was embedded in Leica optimal cutting temperature compound and sectioned. Slides were kept at −80°C and merged in acetone at −20°C for 20 min before staining. Slides were blocked with 2.5% normal goat serum (Vector Laboratories; catalog no. S-1000) at room temperature for 1 h. The slides were incubated with primary antibodies (netrin-1 antibody, LS-C743016, 1:100, LifeSpan BioSciences; anti-neutrophil antibody, ab2557, 1:100, Abcam; cTnT monoclonal antibody, MA5-12960, 1:200, Invitrogen) at 4°C overnight. Conjugated secondary antibody was used to apply the fluorescent dye (Alexa Fluor 546 goat anti-rabbit IgG(H+L), A11010, Invitrogen; Alexa Fluor 488 goat anti-rat IgG(H+L), A11006, Invitrogen; goat anti-mouse IgG(H+L) Highly Cross-Adsorbed Secondary Antibody, Alexa Fluor 647, A21236, Invitrogen; 1:200). The human neutrophils were processed with cytospin (Hettich ROTOFIX 32A centrifuge) and fixed with 4% PFA for 20 min at room temperature. Following blocking with Background Sniper (Biocare Medical; catalog no. BS966L) at room temperature for 1 h, the slides were incubated with primary antibody (rabbit anti-netrin-1, 1:25, catalog no. LS-C743016, LifeSpan BioSciences; mouse anti-human lysozyme, 1:200, Novus Biologicals, catalog no. NB100-63062) at 4°C overnight. Negative control slices were incubated with the recombinant rabbit IgG and mouse IgG (Abcam, catalog no. ab172730; Novus Biologicals, catalog no. NBP1-97019). Conjugated secondary antibody (Alexa Fluor 647 donkey anti-rabbit IgG(H+L), 1:200, Invitrogen, catalog no. A-31573; Alexa Fluor 488 donkey anti-mouse IgG(H+L), 1:200, Invitrogen, catalog no. A32766TR) were used to apply the fluorescence by incubating at room temperature for 1 h. Slides were mounted after counterstaining with DAPI. Images were acquired with a Leica TCS SPE confocal system and Leica DMi8 microscope under a 63× oil lens and processed with ImageJ.

Statistical analysis

GraphPad Prism 7.0 was used for statistical analysis. We report two-sided P values. Statistical significance was accepted at a level of P values <0.05. All data were summarized as mean ± SD. We used the robust nonlinear regression method, which was built into Prism, to detect outliers. One outlier was identified and removed from analysis. We conducted the Kolmogorov–Smirnov test on data of all experiments to examine normal distributions. When the normality assumption held, we used two-sample *t* tests to compare means in the context of equal variance (determined by *F* test) and Welch's *t* tests for data with significantly different variances. The Mann-Whitney test was used to compare medians for data of skewed distributions. For the experiments including more than two groups, besides testing for normality, we conducted the Brown-Forsythe test to examine equal variances. The normality and equal-variance assumptions were tested to be satisfactory. We used the ANOVA method to analyze data and applied the Bonferroni adjustment in the post hoc tests. A statistician reviewed all the data analysis.

Online supplemental material

Fig. S1 shows murine heart tissue netrin-1 protein levels and female and male murine serum netrin-1 levels. Fig. S2 shows immunohistochemical staining for cardiac netrin-1 in WT mice after IR surgery, negative controls for Fig. 1 G, negative controls for Fig. 3 H, murine blood monocyte cell counts after clodronate depletion, and blood netrin-1 levels of WT (C57BL/6) mice with clodronate monocyte/macrophage depletion. Fig. S3 shows the confirmation of netrin-1 knock-down of *Ntnl*$^{loxP/loxP}$ Myosin Cre^{+} mice. Fig. S4 shows treatment effects of different dosages of netrin-1, treatment effects of netrin-1 at different time points, and serum and heart tissue adenosine levels after netrin-1 treatment at different time points. Fig. S5 shows the results of the murine and human neutrophil transmigration assays. Table S1 lists characteristics of patients with MI. Table S2 lists characteristics of healthy donors.

Acknowledgments

We acknowledge Yanyu Wang and Constance L. Atkins for data folder review; Xuebo Chen for maintaining the experimental animals; Jessica L. Bowser for scientific discussions; Hsin-Yi Lu, Shixia Huang, and Yiling Lu for providing the laser scanner; Meng Wang for technical assistance; and Kelli Wallen and Kathy Franz for assisting with the text review and manuscript submission.

The present studies were supported by National Institutes of Health grants R01HL154720, R01DK122796, R01DK109574, and R01HL133900 and U.S. Department of Defense grant W81XWH2110032 to H.K. Eltzschig and Deutsche Forschungsgemeinschaft grant CO 2096/1-1 to C. Conrad.

Author contributions: All authors contributed to the drafting or revising of this work and contributed to the intellectual content. All authors provided final approval of the submitted version and are in agreement to be accountable for all aspects of the work. J. Li designed, performed, and analyzed experiments; prepared the figures; and wrote the manuscript. C. Conrad, T.W. Mills, N.K. Berg, B. Kim, W. Ruan, J.W. Lee, and X. Yuan helped with experiments and amended the manuscript. X. Zhang helped with data analysis and amended the manuscript. H.K. Eltzschig designed experiments and helped with writing the manuscript.

Disclosures: The authors declare no competing interests exist.

Submitted: 2 January 2021
Revised: 26 February 2021
Accepted: 19 March 2021

References

Ackers-Johnson, M., P.Y. Li, A.P. Holmes, S.M. O'Brien, D. Pavlovic, and R.S. Foo. 2016. A simplified, Langendorff-free method for concomitant isolation of viable cardiac myocytes and nonmyocytes from the adult mouse heart. *Circ. Res.* 119:909–920. https://doi.org/10.1161/CIRCRESAHA.116.309202

Aherne, C.M., C.B. Collins, J.C. Masterson, M. Tizzano, T.A. Boyle, J.A. Westrich, J.A. Parnes, G.T. Furuta, J. Rivera-Nieves, and H.K. Eltzschig. 2012. Neuronal guidance molecule netrin-1 attenuates inflammatory cell trafficking during acute experimental colitis. *Gut.* 61:695–705. https://doi.org/10.1136/gutjnl-2011-300012

Aherne, C.M., C.B. Collins, and H.K. Eltzschig. 2013. Netrin-1 guides inflammatory cell migration to control mucosal immune responses during intestinal inflammation. *Tissue Barriers.* 1:e24957. https://doi.org/10.4161/tisb.24957

Aherne, C.M., B. Saeedi, C.B. Collins, J.C. Masterson, E.N. McNamee, L. Perrenoud, C.R. Rapp, V.F. Curtis, A. Bayless, A. Fletcher, et al. 2015. Epithelial-specific A2B adenosine receptor signaling protects the colonic epithelial barrier during acute colitis. *Mucosal Immunol.* 8:1324–1338. https://doi.org/10.1038/mi.2015.22

Alva, J.A., A.C. Zovein, A. Monvoisin, T. Murphy, A. Salazar, N.L. Harvey, P. Carmeliet, and M.L. Iruela-Arispe. 2006. VE-Cadherin-Cre-recombinase transgenic mouse: a tool for lineage analysis and gene deletion in endothelial cells. *Dev. Dyn.* 235:759–767. https://doi.org/10.1002/dvdy.20643

Berg, N.K., J. Li, B. Kim, T. Mills, G. Pei, Z. Zhao, X. Li, X. Zhang, W. Ruan, H.K. Eltzschig, and X. Yuan. 2021. Hypoxia-inducible factor-dependent induction of myeloid-derived netrin-1 attenuates natural killer cell infiltration during endotoxin-induced lung injury. *FASEB J.* 35:e21334. https://doi.org/10.1096/fj.202002407R

Bin, J.M., D. Han, K. Lai Wing Sun, L.P. Croteau, E. Dumontier, J.F. Cloutier, A. Kania, and T.E. Kennedy. 2015. Complete loss of netrin-1 results in embryonic lethality and severe axon guidance defects without increased neural cell death. *Cell Rep.* 12:1099–1106. https://doi.org/10.1016/j.celrep.2015.07.028

Bonaventura, A., F. Montecucco, and F. Dallegri. 2016. Cellular recruitment in myocardial ischaemia/reperfusion injury. *Eur. J. Clin. Invest.* 46:590–601. https://doi.org/10.1111/eci.12633

Bouhidel, J.O., P. Wang, K.L. Siu, H. Li, J.Y. Youn, and H. Cai. 2015. Netrin-1 improves post-injury cardiac function in vivo via DCC/NO-dependent preservation of mitochondrial integrity, while attenuating autophagy. *Biochim. Biophys. Acta.* 1852:277–289. https://doi.org/10.1016/j.bbadis.2014.06.005

Brunet, I., E. Gordon, J. Han, B. Cristofaro, D. Broqueres-You, C. Liu, K. Bouvrée, J. Zhang, R. del Toro, T. Mathivet, et al. 2014. Netrin-1 controls sympathetic arterial innervation. *J. Clin. Invest.* 124:3230–3240. https://doi.org/10.1172/JCI75181

Cai, Z., H. Zhong, M. Bosch-Marce, K. Fox-Talbot, L. Wang, C. Wei, M.A. Trush, and G.L. Semenza. 2008. Complete loss of ischaemic preconditioning-induced cardioprotection in mice with partial deficiency of HIF-1 α. *Cardiovasc. Res.* 77:463–470. https://doi.org/10.1093/cvr/cvm035

Cai, Z., W. Luo, H. Zhan, and G.L. Semenza. 2013. Hypoxia-inducible factor 1 is required for remote ischemic preconditioning of the heart. *Proc. Natl. Acad. Sci. USA.* 110:17462–17467. https://doi.org/10.1073/pnas.1317158110

Clausen, B.E., C. Burkhardt, W. Reith, R. Renkawitz, and I. Förster. 1999. Conditional gene targeting in macrophages and granulocytes using LysMcre mice. *Transgenic Res.* 8:265–277. https://doi.org/10.1023/A:1008942828960

Corset, V., K.T. Nguyen-Ba-Charvet, C. Forcet, E. Moyse, A. Chédotal, and P. Mehlen. 2000. Netrin-1-mediated axon outgrowth and cAMP production requires interaction with adenosine A2b receptor. *Nature.* 407:747–750. https://doi.org/10.1038/35037600

Duan, L., B.L. Woolbright, H. Jaeschke, and A. Ramachandran. 2020. Late protective effect of netrin-1 in the murine acetaminophen hepatotoxicity model. *Toxicol. Sci.* 175:168–181. https://doi.org/10.1093/toxsci/kfaa041

Eckle, T., A. Grenz, D. Köhler, A. Redel, M. Falk, B. Rolauffs, H. Osswald, F. Kehl, and H.K. Eltzschig. 2006. Systematic evaluation of a novel model for cardiac ischemic preconditioning in mice. *Am. J. Physiol. Heart Circ. Physiol.* 291:H2533–H2540. https://doi.org/10.1152/ajpheart.00472.2006

Eckle, T., T. Krahn, A. Grenz, D. Köhler, M. Mittelbronn, C. Ledent, M.A. Jacobson, H. Osswald, L.F. Thompson, K. Unertl, and H.K. Eltzschig. 2007. Cardioprotection by ecto-5′-nucleotidase (CD73) and A2B adenosine receptors. *Circulation.* 115:1581–1590. https://doi.org/10.1161/CIRCULATIONAHA.106.669697

Eckle, T., M. Faigle, A. Grenz, S. Laucher, L.F. Thompson, and H.K. Eltzschig. 2008a. A2B adenosine receptor dampens hypoxia-induced vascular leak. *Blood.* 111:2024–2035. https://doi.org/10.1182/blood-2007-10-117044

Eckle, T., A. Grenz, S. Laucher, and H.K. Eltzschig. 2008b. A2B adenosine receptor signaling attenuates acute lung injury by enhancing alveolar fluid clearance in mice. *J. Clin. Invest.* 118:3301–3315. https://doi.org/10.1172/JCI34203

Eckle, T., D. Köhler, R. Lehmann, K. El Kasmi, and H.K. Eltzschig. 2008c. Hypoxia-inducible factor-1 is central to cardioprotection: a new paradigm for ischemic preconditioning. *Circulation.* 118:166–175. https://doi.org/10.1161/CIRCULATIONAHA.107.758516

Eckle, T., M. Koeppen, and H. Eltzschig. 2011. Use of a hanging weight system for coronary artery occlusion in mice. *J. Vis. Exp.* (50):2526. https://doi.org/10.3791/2526

Eckle, T., K. Hartmann, S. Bonney, S. Reithel, M. Mittelbronn, L.A. Walker, B.D. Lowes, J. Han, C.H. Borchers, P.M. Buttrick, et al. 2012. Adora2b-elicited Per2 stabilization promotes a HIF-dependent metabolic switch crucial for myocardial adaptation to ischemia. *Nat. Med.* 18:774–782. https://doi.org/10.1038/nm.2728

Eckle, T., K. Hughes, H. Ehrentraut, K.S. Brodsky, P. Rosenberger, D.S. Choi, K. Ravid, T. Weng, Y. Xia, M.R. Blackburn, and H.K. Eltzschig. 2013. Crosstalk between the equilibrative nucleoside transporter ENT2 and alveolar Adora2b adenosine receptors dampens acute lung injury. *FASEB J.* 27:3078–3089. https://doi.org/10.1096/fj.13-228551

Eltzschig, H.K., T. Eckle, A. Mager, N. Küper, C. Karcher, T. Weissmüller, K. Boengler, R. Schulz, S.C. Robson, and S.P. Colgan. 2006. ATP release from activated neutrophils occurs via connexin 43 and modulates adenosine-dependent endothelial cell function. *Circ. Res.* 99:1100–1108. https://doi.org/10.1161/01.RES.0000250174.31269.70

Eltzschig, H.K., C.F. Macmanus, and S.P. Colgan. 2008. Neutrophils as sources of extracellular nucleotides: functional consequences at the vascular interface. *Trends Cardiovasc. Med.* 18:103–107. https://doi.org/10.1016/j.tcm.2008.01.006

Eltzschig, H.K., M.V. Sitkovsky, and S.C. Robson. 2012. Purinergic signaling during inflammation. *N. Engl. J. Med.* 367:2322–2333. https://doi.org/10.1056/NEJMra1205750

Eltzschig, H.K., S.K. Bonney, and T. Eckle. 2013. Attenuating myocardial ischemia by targeting A2B adenosine receptors. *Trends Mol. Med.* 19:345–354. https://doi.org/10.1016/j.molmed.2013.02.005

Faurschou, M., and N. Borregaard. 2003. Neutrophil granules and secretory vesicles in inflammation. *Microbes Infect.* 5:1317–1327. https://doi.org/10.1016/j.micinf.2003.09.008

Feinstein, J., and B. Ramkhelawon. 2017. Netrins & Semaphorins: Novel regulators of the immune response. *Biochim. Biophys. Acta Mol. Basis Dis.* 1863:3183–3189. https://doi.org/10.1016/j.bbadis.2017.09.010

Ferrari, D., E.N. McNamee, M. Idzko, R. Gambari, and H.K. Eltzschig. 2016. Purinergic signaling during immune cell trafficking. *Trends Immunol.* 37:399–411. https://doi.org/10.1016/j.it.2016.04.004

Frangogiannis, N.G. 2014. The inflammatory response in myocardial injury, repair, and remodelling. *Nat. Rev. Cardiol.* 11:255–265. https://doi.org/10.1038/nrcardio.2014.28

Grenz, A., J.H. Dalton, J.D. Bauerle, A. Badulak, D. Ridyard, A. Gandjeva, C.M. Aherne, K.S. Brodsky, J.H. Kim, R.M. Tuder, and H.K. Eltzschig. 2011a. Partial netrin-1 deficiency aggravates acute kidney injury. *PLoS One.* 6:e14812. https://doi.org/10.1371/journal.pone.0014812

Grenz, A., D. Homann, and H.K. Eltzschig. 2011b. Extracellular adenosine: a safety signal that dampens hypoxia-induced inflammation during ischemia. *Antioxid. Redox Signal.* 15:2221–2234. https://doi.org/10.1089/ars.2010.3665

Guan, K.L., and Y. Rao. 2003. Signalling mechanisms mediating neuronal responses to guidance cues. *Nat. Rev. Neurosci.* 4:941–956. https://doi.org/10.1038/nrn1254

Hadi, T., L. Boytard, M. Silvestro, D. Alebrahim, S. Jacob, J. Feinstein, K. Barone, W. Spiro, S. Hutchison, R. Simon, et al. 2018. Macrophage-derived netrin-1 promotes abdominal aortic aneurysm formation by activating MMP3 in vascular smooth muscle cells. *Nat. Commun.* 9:5022. https://doi.org/10.1038/s41467-018-07495-1

Hansen, P.R. 1995. Role of neutrophils in myocardial ischemia and reperfusion. *Circulation.* 91:1872–1885. https://doi.org/10.1161/01.CIR.91.6.1872

Haskó, G., and B.N. Cronstein. 2004. Adenosine: an endogenous regulator of innate immunity. *Trends Immunol.* 25:33–39. https://doi.org/10.1016/j.it.2003.11.003

Haskó, G., J. Linden, B. Cronstein, and P. Pacher. 2008. Adenosine receptors: therapeutic aspects for inflammatory and immune diseases. *Nat. Rev. Drug Discov.* 7:759–770. https://doi.org/10.1038/nrd2638

Haskó, G., B. Csóka, Z.H. Németh, E.S. Vizi, and P. Pacher. 2009. $A_{(2B)}$ adenosine receptors in immunity and inflammation. *Trends Immunol.* 30:263–270. https://doi.org/10.1016/j.it.2009.04.001

Hausenloy, D.J., and D.M. Yellon. 2013. Myocardial ischemia-reperfusion injury: a neglected therapeutic target. *J. Clin. Invest.* 123:92–100. https://doi.org/10.1172/JCI62874

Hausenloy, D.J., H.E. Botker, T. Engstrom, D. Erlinge, G. Heusch, B. Ibanez, R.A. Kloner, M. Ovize, D.M. Yellon, and D. Garcia-Dorado. 2017. Targeting reperfusion injury in patients with ST-segment elevation myocardial infarction: trials and tribulations. *Eur. Heart J.* 38:935–941.

He, J., Y. Zhao, W. Deng, and D.X. Wang. 2014. Netrin-1 promotes epithelial sodium channel-mediated alveolar fluid clearance via activation of the adenosine 2B receptor in lipopolysaccharide-induced acute lung injury. *Respiration.* 87:394–407. https://doi.org/10.1159/000358066

Heusch, G. 2020. Myocardial ischaemia-reperfusion injury and cardioprotection in perspective. *Nat. Rev. Cardiol.* 17:773–789. https://doi.org/10.1038/s41569-020-0403-y

Hoegl, S., K.S. Brodsky, M.R. Blackburn, H. Karmouty-Quintana, B. Zwissler, and H.K. Eltzschig. 2015. Alveolar epithelial A2B adenosine receptors in pulmonary protection during acute lung injury. *J. Immunol.* 195:1815–1824. https://doi.org/10.4049/jimmunol.1401957

Idzko, M., D. Ferrari, and H.K. Eltzschig. 2014. Nucleotide signalling during inflammation. *Nature.* 509:310–317. https://doi.org/10.1038/nature13085

Kalogeris, T., C.P. Baines, M. Krenz, and R.J. Korthuis. 2012. Cell biology of ischemia/reperfusion injury. *Int. Rev. Cell Mol. Biol.* 298:229–317. https://doi.org/10.1016/B978-0-12-394309-5.00006-7

Keller, M., V. Mirakaj, M. Koeppen, and P. Rosenberger. 2021. Neuronal guidance proteins in cardiovascular inflammation. *Basic Res. Cardiol.* 116:6. https://doi.org/10.1007/s00395-021-00847-x

Koeppen, M., T. Eckle, and H.K. Eltzschig. 2009. Selective deletion of the A1 adenosine receptor abolishes heart-rate slowing effects of intravascular adenosine in vivo. *PLoS One.* 4:e6784. https://doi.org/10.1371/journal.pone.0006784

Koeppen, M., J.W. Lee, S.W. Seo, K.S. Brodsky, S. Kreth, I.V. Yang, P.M. Buttrick, T. Eckle, and H.K. Eltzschig. 2018. Hypoxia-inducible factor 2-alpha-dependent induction of amphiregulin dampens myocardial ischemia-reperfusion injury. *Nat. Commun.* 9:816. https://doi.org/10.1038/s41467-018-03105-2

Köhler, D., T. Eckle, M. Faigle, A. Grenz, M. Mittelbronn, S. Laucher, M.L. Hart, S.C. Robson, C.E. Müller, and H.K. Eltzschig. 2007. CD39/ectonucleoside triphosphate diphosphohydrolase 1 provides myocardial protection during cardiac ischemia/reperfusion injury. *Circulation.* 116:1784–1794. https://doi.org/10.1161/CIRCULATIONAHA.107.690180

Köhler, D., A. Streißenberger, K. König, T. Granja, J.M. Roth, R. Lehmann, C.B. de Oliveira Franz, and P. Rosenberger. 2013. The uncoordinated-5 homolog B (UNC5B) receptor increases myocardial ischemia-reperfusion injury. *PLoS One.* 8:e69477. https://doi.org/10.1371/journal.pone.0069477

Köhler, D., T. Granja, J. Volz, M. Koeppen, H.F. Langer, G. Hansmann, E. Legchenko, T. Geisler, T. Bakchoul, C. Eggstein, et al. 2020. Red blood cell-derived semaphorin 7A promotes thrombo-inflammation in myocardial ischemia-reperfusion injury through platelet GPIb. *Nat. Commun.* 11:1315. https://doi.org/10.1038/s41467-020-14958-x

Kolaczkowska, E., and P. Kubes. 2013. Neutrophil recruitment and function in health and inflammation. *Nat. Rev. Immunol.* 13:159–175. https://doi.org/10.1038/nri3399

Körner, A., M. Schlegel, T. Kaussen, V. Gudernatsch, G. Hansmann, T. Schumacher, M. Giera, and V. Mirakaj. 2019. Sympathetic nervous system controls resolution of inflammation via regulation of repulsive guidance molecule A. *Nat. Commun.* 10:633. https://doi.org/10.1038/s41467-019-08328-5

Layne, K., A. Ferro, and G. Passacquale. 2015. Netrin-1 as a novel therapeutic target in cardiovascular disease: to activate or inhibit? *Cardiovasc. Res.* 107:410–419. https://doi.org/10.1093/cvr/cvv201

Lee, J.W., M. Koeppen, S.W. Seo, J.L. Bowser, X. Yuan, J. Li, M. Sibilia, A.V. Ambardekar, X. Zhang, T. Eckle, et al. 2020. Transcription-independent induction of ERBB1 through hypoxia-inducible factor 2A provides cardioprotection during ischemia and reperfusion. *Anesthesiology.* 132:763–780. https://doi.org/10.1097/ALN.0000000000003037

Li, Q., P. Wang, K. Ye, and H. Cai. 2015. Central role of SIAH inhibition in DCC-dependent cardioprotection provoked by netrin-1/NO. *Proc. Natl. Acad. Sci. USA.* 112:899–904. https://doi.org/10.1073/pnas.1420695112

Mao, X., H. Xing, A. Mao, H. Jiang, L. Cheng, Y. Liu, X. Quan, and L. Li. 2014. Netrin-1 attenuates cardiac ischemia reperfusion injury and generates alternatively activated macrophages. *Inflammation.* 37:573–580. https://doi.org/10.1007/s10753-013-9771-3

Matherne, G.P., J. Linden, A.M. Byford, N.S. Gauthier, and J.P. Headrick. 1997. Transgenic A1 adenosine receptor overexpression increases myocardial resistance to ischemia. *Proc. Natl. Acad. Sci. USA.* 94:6541–6546. https://doi.org/10.1073/pnas.94.12.6541

Mirakaj, V., and P. Rosenberger. 2017. Immunomodulatory functions of neuronal guidance proteins. *Trends Immunol.* 38:444–456. https://doi.org/10.1016/j.it.2017.03.007

Mirakaj, V., C.A. Thix, S. Laucher, C. Mielke, J.C. Morote-Garcia, M.A. Schmit, J. Henes, K.E. Unertl, D. Köhler, and P. Rosenberger. 2010. Netrin-1 dampens pulmonary inflammation during acute lung injury. *Am. J. Respir. Crit. Care Med.* 181:815–824. https://doi.org/10.1164/rccm.200905-0717OC

Mirakaj, V., D. Gatidou, C. Pötzsch, K. König, and P. Rosenberger. 2011. Netrin-1 signaling dampens inflammatory peritonitis. *J. Immunol.* 186: 549–555. https://doi.org/10.4049/jimmunol.1002671

Mirakaj, V., J. Dalli, T. Granja, P. Rosenberger, and C.N. Serhan. 2014. Vagus nerve controls resolution and pro-resolving mediators of inflammation. *J. Exp. Med.* 211:1037–1048. https://doi.org/10.1084/jem.20132103

Moore, S.W., M. Tessier-Lavigne, and T.E. Kennedy. 2007. Netrins and their receptors. *Adv. Exp. Med. Biol.* 621:17–31. https://doi.org/10.1007/978-0-387-76715-4_2

Morote-Garcia, J.C., P. Rosenberger, J. Kuhlicke, and H.K. Eltzschig. 2008. HIF-1-dependent repression of adenosine kinase attenuates hypoxia-induced vascular leak. *Blood.* 111:5571–5580. https://doi.org/10.1182/blood-2007-11-126763

Neudecker, V., K.S. Brodsky, E.T. Clambey, E.P. Schmidt, T.A. Packard, B. Davenport, T.J. Standiford, T. Weng, A.A. Fletcher, L. Barthel, et al. 2017. Neutrophil transfer of *miR-223* to lung epithelial cells dampens acute lung injury in mice. *Sci. Transl. Med.* 9:eaah5360. https://doi.org/10.1126/scitranslmed.aah5360

O'Connell, K.E., A.M. Mikkola, A.M. Stepanek, A. Vernet, C.D. Hall, C.C. Sun, E. Yildirim, J.F. Staropoli, J.T. Lee, and D.E. Brown. 2015. Practical murine hematopathology: a comparative review and implications for research. *Comp. Med.* 65:96–113.

Ohta, A., and M. Sitkovsky. 2001. Role of G-protein-coupled adenosine receptors in downregulation of inflammation and protection from tissue damage. *Nature.* 414:916–920. https://doi.org/10.1038/414916a

Poth, J.M., K. Brodsky, H. Ehrentraut, A. Grenz, and H.K. Eltzschig. 2013. Transcriptional control of adenosine signaling by hypoxia-inducible transcription factors during ischemic or inflammatory disease. *J. Mol. Med. (Berl.).* 91:183–193. https://doi.org/10.1007/s00109-012-0988-7

Puhl, S.L., and S. Steffens. 2019. Neutrophils in post-myocardial infarction inflammation: damage vs. resolution? *Front. Cardiovasc. Med.* 6:25. https://doi.org/10.3389/fcvm.2019.00025

Ramesh, G., C.D. Krawczeski, J.G. Woo, Y. Wang, and P. Devarajan. 2010. Urinary netrin-1 is an early predictive biomarker of acute kidney injury after cardiac surgery. *Clin. J. Am. Soc. Nephrol.* 5:395–401. https://doi.org/10.2215/CJN.05140709

Ramkhelawon, B., Y. Yang, J.M. van Gils, B. Hewing, K.J. Rayner, S. Parathath, L. Guo, S. Oldebeken, J.L. Feig, E.A. Fisher, and K.J. Moore. 2013. Hypoxia induces netrin-1 and Unc5b in atherosclerotic plaques: mechanism for macrophage retention and survival. *Arterioscler. Thromb. Vasc. Biol.* 33:1180–1188. https://doi.org/10.1161/ATVBAHA.112.301008

Ranganathan, P., C. Jayakumar, and G. Ramesh. 2013. Proximal tubule-specific overexpression of netrin-1 suppresses acute kidney injury-induced interstitial fibrosis and glomerulosclerosis through suppression of IL-6/STAT3 signaling. *Am. J. Physiol. Renal Physiol.* 304: F1054–F1065. https://doi.org/10.1152/ajprenal.00650.2012

Rosenberger, P., J.M. Schwab, V. Mirakaj, E. Masekowsky, A. Mager, J.C. Morote-Garcia, K. Unertl, and H.K. Eltzschig. 2009. Hypoxia-inducible factor-dependent induction of netrin-1 dampens inflammation caused by hypoxia. *Nat. Immunol.* 10:195–202. https://doi.org/10.1038/ni.1683

Schlegel, M., D. Köhler, A. Körner, T. Granja, A. Straub, M. Giera, and V. Mirakaj. 2016. The neuroimmune guidance cue netrin-1 controls resolution programs and promotes liver regeneration. *Hepatology.* 63: 1689–1705. https://doi.org/10.1002/hep.28347

Schlegel, M., A. Körner, T. Kaussen, U. Knausberg, C. Gerber, G. Hansmann, H.S. Jónasdóttir, M. Giera, and V. Mirakaj. 2018. Inhibition of neogenin fosters resolution of inflammation and tissue regeneration. *J. Clin. Invest.* 128:4711–4726. https://doi.org/10.1172/JCI96259

Schwenk, F., U. Baron, and K. Rajewsky. 1995. A cre-transgenic mouse strain for the ubiquitous deletion of loxP-flanked gene segments including deletion in germ cells. *Nucleic Acids Res.* 23:5080–5081. https://doi.org/10.1093/nar/23.24.5080

Semenza, G.L. 2011. Oxygen sensing, homeostasis, and disease. *N. Engl. J. Med.* 365:537–547. https://doi.org/10.1056/NEJMra1011165

Seo, S.W., M. Koeppen, S. Bonney, M. Gobel, M. Thayer, P.N. Harter, K. Ravid, H.K. Eltzschig, M. Mittelbronn, L. Walker, and T. Eckle. 2015. Differential tissue-specific function of Adora2b in cardioprotection. *J. Immunol.* 195:1732–1743. https://doi.org/10.4049/jimmunol.1402288

Serafini, T., T.E. Kennedy, M.J. Galko, C. Mirzayan, T.M. Jessell, and M. Tessier-Lavigne. 1994. The netrins define a family of axon outgrowth-promoting proteins homologous to *C. elegans* UNC-6. *Cell.* 78:409–424. https://doi.org/10.1016/0092-8674(94)90420-0

Serafini, T., S.A. Colamarino, E.D. Leonardo, H. Wang, R. Beddington, W.C. Skarnes, and M. Tessier-Lavigne. 1996. Netrin-1 is required for commissural axon guidance in the developing vertebrate nervous system. *Cell.* 87:1001–1014. https://doi.org/10.1016/S0092-8674(00)81795-X

Silvestre-Roig, C., Q. Braster, A. Ortega-Gomez, and O. Soehnlein. 2020. Neutrophils as regulators of cardiovascular inflammation. *Nat. Rev. Cardiol.* 17:327–340. https://doi.org/10.1038/s41569-019-0326-7

Sitkovsky, M., and D. Lukashev. 2005. Regulation of immune cells by local-tissue oxygen tension: HIF1 alpha and adenosine receptors. *Nat. Rev. Immunol.* 5:712–721. https://doi.org/10.1038/nri1685

Sitkovsky, M.V., D. Lukashev, S. Apasov, H. Kojima, M. Koshiba, C. Caldwell, A. Ohta, and M. Thiel. 2004. Physiological control of immune response and inflammatory tissue damage by hypoxia-inducible factors and adenosine A2A receptors. *Annu. Rev. Immunol.* 22:657–682. https://doi.org/10.1146/annurev.immunol.22.012703.104731

Siu, K.L., C. Lotz, P. Ping, and H. Cai. 2015. Netrin-1 abrogates ischemia/reperfusion-induced cardiac mitochondrial dysfunction via nitric oxide-dependent attenuation of NOX4 activation and recoupling of NOS. *J. Mol. Cell. Cardiol.* 78:174–185. https://doi.org/10.1016/j.yjmcc.2014.07.005

Smith, C.W., M.L. Entman, C.L. Lane, A.L. Beaudet, T.I. Ty, K. Youker, H.K. Hawkins, and D.C. Anderson. 1991. Adherence of neutrophils to canine cardiac myocytes in vitro is dependent on intercellular adhesion molecule-1. *J. Clin. Invest.* 88:1216–1223. https://doi.org/10.1172/JCI115424

Sohal, D.S., M. Nghiem, M.A. Crackower, S.A. Witt, T.R. Kimball, K.M. Tymitz, J.M. Penninger, and J.D. Molkentin. 2001. Temporally regulated and tissue-specific gene manipulations in the adult and embryonic heart using a tamoxifen-inducible Cre protein. *Circ. Res.* 89:20–25. https://doi.org/10.1161/hh1301.092687

Stein, E., Y. Zou, M. Poo, and M. Tessier-Lavigne. 2001. Binding of DCC by netrin-1 to mediate axon guidance independent of adenosine A2B receptor activation. *Science.* 291:1976–1982. https://doi.org/10.1126/science.1059391

Thiel, M., A. Chouker, A. Ohta, E. Jackson, C. Caldwell, P. Smith, D. Lukashev, I. Bittmann, and M.V. Sitkovsky. 2005. Oxygenation inhibits the physiological tissue-protecting mechanism and thereby exacerbates acute inflammatory lung injury. *PLoS Biol.* 3:e174. https://doi.org/10.1371/journal.pbio.0030174

Van Battum, E.Y., S. Brignani, and R.J. Pasterkamp. 2015. Axon guidance proteins in neurological disorders. *Lancet Neurol.* 14:532–546. https://doi.org/10.1016/S1474-4422(14)70257-1

van Gils, J.M., M.C. Derby, L.R. Fernandes, B. Ramkhelawon, T.D. Ray, K.J. Rayner, S. Parathath, E. Distel, J.L. Feig, J.I. Alvarez-Leite, et al. 2012. The neuroimmune guidance cue netrin-1 promotes atherosclerosis by inhibiting the emigration of macrophages from plaques. *Nat. Immunol.* 13:136–143. https://doi.org/10.1038/ni.2205

Varadarajan, S.G., J.H. Kong, K.D. Phan, T.J. Kao, S.C. Panaitof, J. Cardin, H. Eltzschig, A. Kania, B.G. Novitch, and S.J. Butler. 2017. Netrin1 produced by neural progenitors, not floor plate cells, is required for axon guidance in the spinal cord. *Neuron.* 94:790–799.e3. https://doi.org/10.1016/j.neuron.2017.03.007

Vinten-Johansen, J. 2004. Involvement of neutrophils in the pathogenesis of lethal myocardial reperfusion injury. *Cardiovasc. Res.* 61:481–497. https://doi.org/10.1016/j.cardiores.2003.10.011

Wakamiya, M., M.R. Blackburn, R. Jurecic, M.J. McArthur, R.S. Geske, J. Cartwright Jr., K. Mitani, S. Vaishnav, J.W. Belmont, R.E. Kellems, et al. 1995. Disruption of the adenosine deaminase gene causes hepatocellular impairment and perinatal lethality in mice. *Proc. Natl. Acad. Sci. USA.* 92: 3673–3677. https://doi.org/10.1073/pnas.92.9.3673

Wang, G.L., and G.L. Semenza. 1993. Characterization of hypoxia-inducible factor 1 and regulation of DNA binding activity by hypoxia. *J. Biol. Chem.* 268:21513–21518. https://doi.org/10.1016/S0021-9258(20)80571-7

Wang, G.L., B.H. Jiang, E.A. Rue, and G.L. Semenza. 1995. Hypoxia-inducible factor 1 is a basic-helix-loop-helix-PAS heterodimer regulated by cellular O_2 tension. *Proc. Natl. Acad. Sci. USA.* 92:5510–5514. https://doi.org/10.1073/pnas.92.12.5510

Yellon, D.M., and D.J. Hausenloy. 2007. Myocardial reperfusion injury. *N. Engl. J. Med.* 357:1121–1135. https://doi.org/10.1056/NEJMra071667

Yuan, X., N. Berg, J.W. Lee, T.T. Le, V. Neudecker, N. Jing, and H. Eltzschig. 2018. MicroRNA miR-223 as regulator of innate immunity. *J. Leukoc. Biol.* 104:515–524. https://doi.org/10.1002/JLB.3MR0218-079R

Zhang, J., and H. Cai. 2010. Netrin-1 prevents ischemia/reperfusion-induced myocardial infarction via a DCC/ERK1/2/eNOS s1177/NO/DCC feed-forward mechanism. *J. Mol. Cell. Cardiol.* 48:1060–1070. https://doi.org/10.1016/j.yjmcc.2009.11.020

Zhang, Y., P. Chen, G. Di, X. Qi, Q. Zhou, and H. Gao. 2018. Netrin-1 promotes diabetic corneal wound healing through molecular mechanisms mediated via the adenosine 2B receptor. *Sci. Rep.* 8:5994. https://doi.org/10.1038/s41598-018-24506-9

Zhu, S., J. Zhu, G. Zhen, Y. Hu, S. An, Y. Li, Q. Zheng, Z. Chen, Y. Yang, M. Wan, et al. 2019. Subchondral bone osteoclasts induce sensory innervation and osteoarthritis pain. *J. Clin. Invest.* 129:1076–1093. https://doi.org/10.1172/JCI121561

Supplemental material

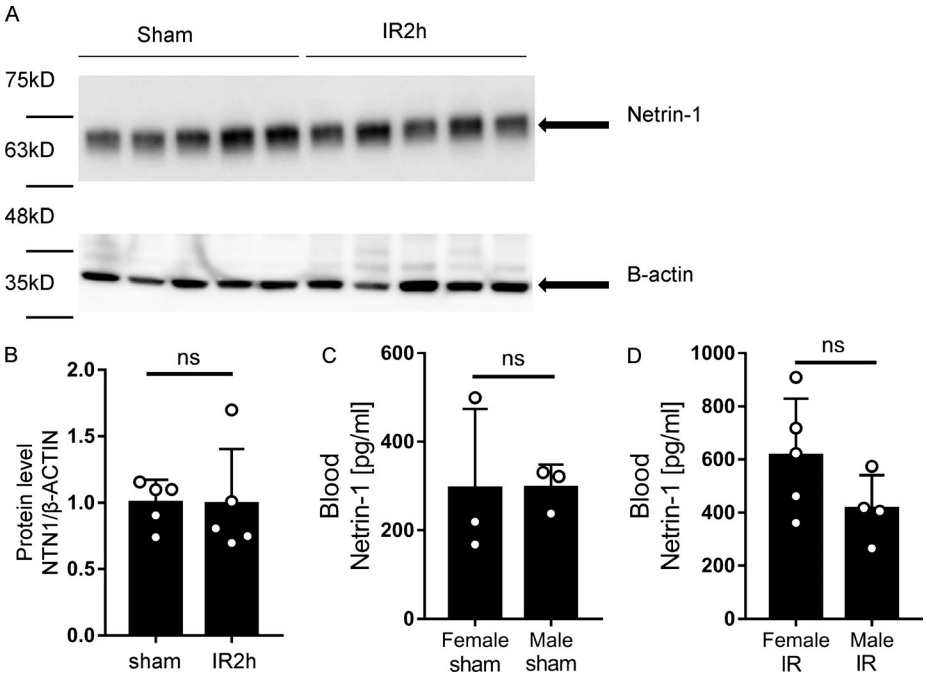

Figure S1. **Netrin-1 levels showed no differences in murine IR heart tissue and blood of female/male subgroups. (A and B)** Murine heart tissue netrin-1 levels were measured in sham and IR2h groups with Western blot analysis. Quantifications showed netrin-1 levels in heart tissue did not change significantly after 45 min of ischemia and 2 h of reperfusion (n = 5 for each group; two-tailed unpaired t test). **(C and D)** Murine IR injury model shows no significant differences of blood netrin-1 levels between female and male mice in both sham and IR groups (n = 3 per sham group, n = 5 for female IR group, and n = 4 for male IR group; two-tailed unpaired t test). Data are presented as mean ± SD.

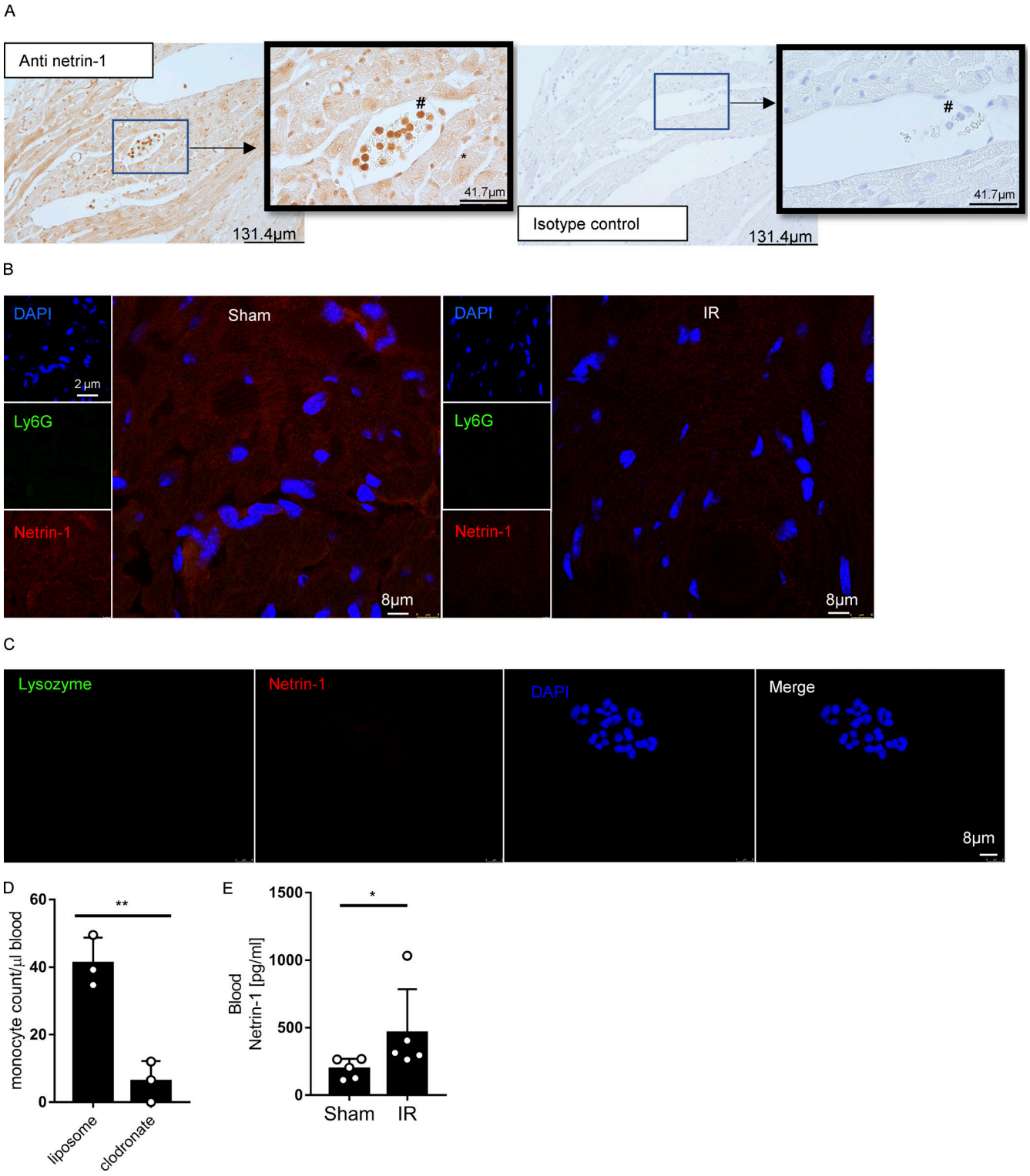

Figure S2. **Netrin-1 staining of heart tissue, negative controls of immunofluorecence, and blood netrin-1 levels of monocyte/macrophage-depleted mice. (A)** Immunohistochemical staining for cardiac netrin-1 in WT mice after IR surgery shows positive staining in cardiomyocytes and neutrophils (n = 3; *, cardiomyocytes; #, neutrophils; for original pictures, scale bar = 131.8 μm; for enlarged pictures, scale bar = 41.7 μm). **(B)** Negative controls for Fig. 1 G (for single-channel pictures, scale bar = 2 μm; for merged channel pictures, scale bar = 8 μm). **(C)** Negative controls for Fig. 3 H. Scale bar = 10 μm. **(D)** Murine blood monocyte cell counts after clodronate depletion compared with liposome control group (n = 3 for each group; two-tailed unpaired t test). **(E)** Blood netrin-1 levels of WT (C57BL/6) mice with clodronate monocyte/macrophage depletion after IR surgery compared with sham group (n = 5 for each group; Mann-Whitney test). *, $P < 0.05$; **, $P < 0.01$. Data are presented as mean ± SD.

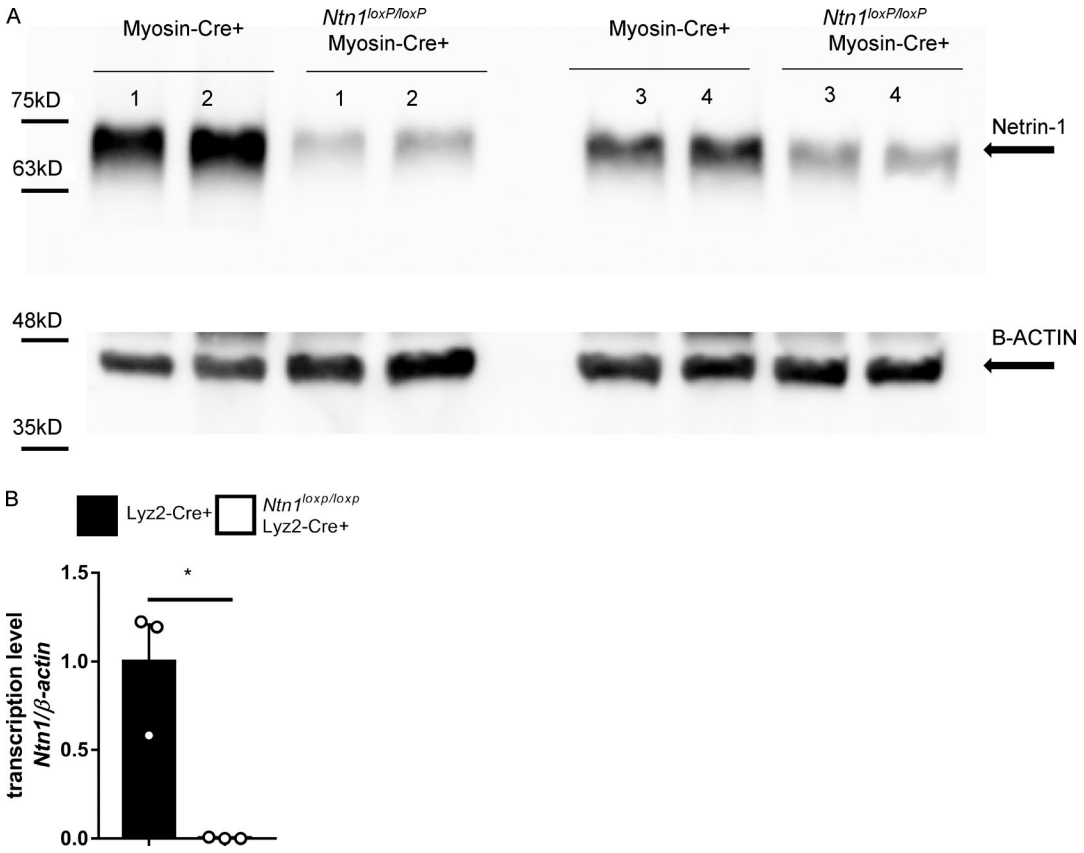

Figure S3. **Confirmations of tissue-specific netrin-1 knock-down mice. (A)** Representative Western blot shows the confirmation of netrin-1 knock-down in heart tissue of *Ntn1*$^{loxP/loxP}$ Myosin Cre^{+} mice (n = 4). **(B)** Netrin-1 transcription levels of bone marrow cells determined by RT-qPCR show netrin-1 knock-down in the myeloid compartment of *Ntn1*$^{loxP/loxP}$ Lyz2 Cre^{+} mice (n = 3; two-tailed Welch's t test; *, P < 0.05. Data are presented as mean ± SD).

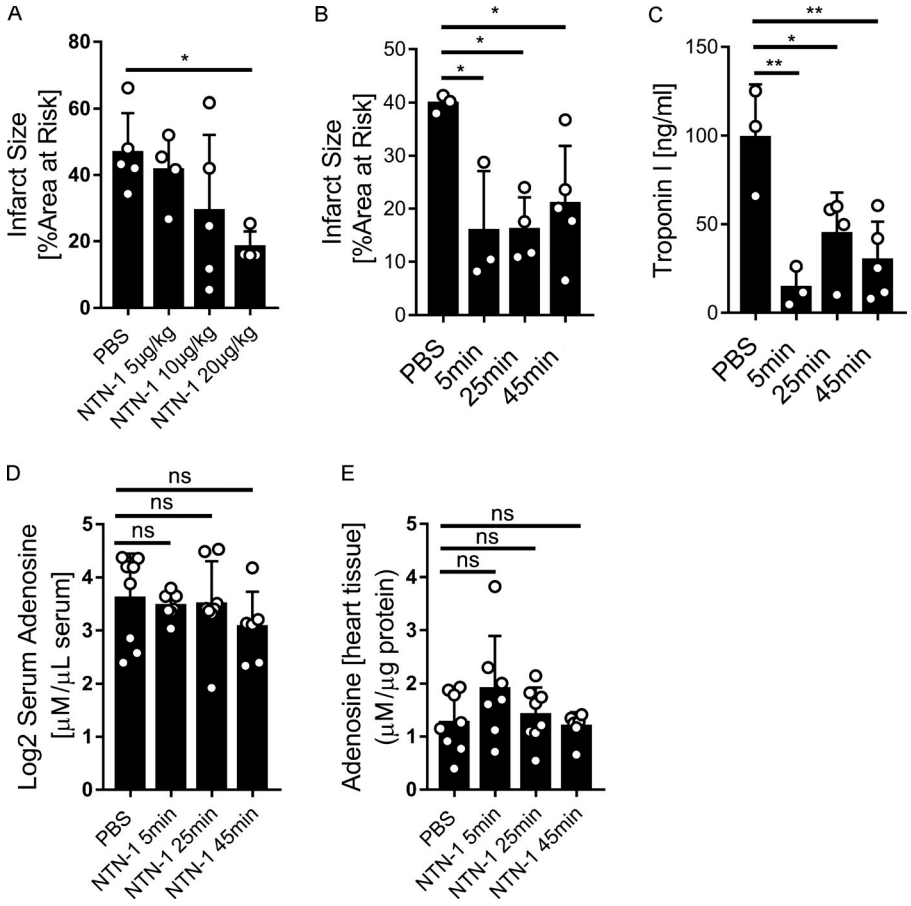

Figure S4. **Therapeutic effects of netrin-1 given in different dosages or time points and adenosine levels changes after netrin-1 treatment. (A)** Recombinant mouse netrin-1 (NTN1) was given to WT mice 5 min before reperfusion during IR surgery at different dosages (5 μg/kg, 10 μg/kg, and 20 μg/kg, equal volumes of PBS as control). Infarct sizes showed that 20 μg/kg netrin-1 presented significant cardioprotection (n = 5 for PBS group, n = 4 for 5 μg/kg group, n = 5 for 10 μg/kg group, and n = 4 for 20 μg/kg group; one-way ANOVA with Bonferroni post hoc tests). **(B and C)** Recombinant mouse netrin-1 (NTN1) was given to WT mice 5 min, 25 min, or 45 min before reperfusion during IR surgery (20 μg/kg or equal volume of PBS). Infarct sizes (B) and troponin levels (C) showed protective effects from three different treatment time points. **(D and E)** Mouse serum adenosine levels and heart tissue adenosine levels showed no significant changes after netrin-1 treatment (20 μg/kg netrin-1; adenosine levels were measured at 5 min, 25 min, and 45 min after netrin-1 injection via HPLC). *, P < 0.05; **, P < 0.01. Data are presented as mean ± SD.

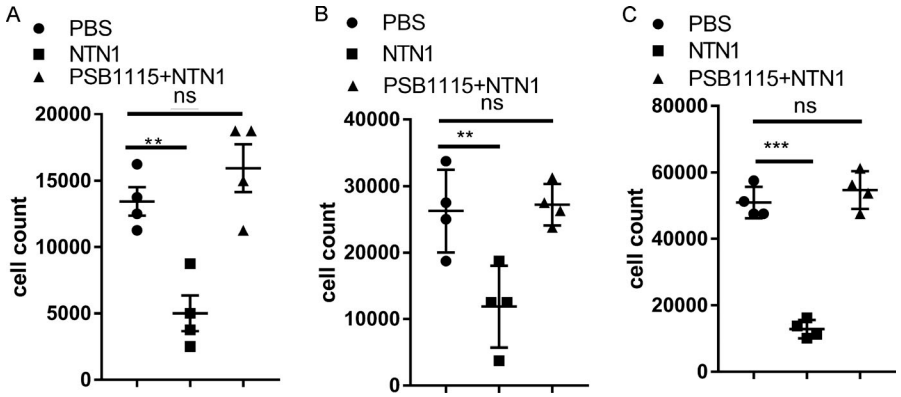

Figure S5. **Netrin-1 reduces neutrophil transmigration, which is ADORA2B dependent. (A)** Murine neutrophil transmigration assay results show NTN1 reduces murine neutrophil transmigration and ADORA2B receptor antagonist PSB1115 abolishes the effect (n = 4 per group; one-way ANOVA with Bonferroni post hoc tests). Data from four independent experiments. **(B and C)** Human neutrophil transmigration assay 1-h (B) and 2-h (C) results show NTN1 reduces human neutrophil transmigration and ADORA2B receptor antagonist PSB1115 abolishes the effect (n = 4 per group; one-way ANOVA with Bonferroni post hoc tests). **, P < 0.01; ***, P < 0.001. Data are presented as mean ± SD. Data from four independent experiments.

Provided online are two tables. Table S1 lists characteristics of patients with MI. Table S2 lists characteristics of healthy donors.